



ESA CONTRACT REPORT

Contract Report to the European Space Agency

**The technical support for global
validation of ERS Wind and Wave
Products at ECMWF
(April 2004 – June 2006)**

August 2006

Authors: Saleh Abdalla and Hans Hersbach

Final report for ESA contract 18212/04/I-OL

European Centre for Medium-Range Weather Forecasts
Europäisches Zentrum für mittelfristige Wettervorhersage
Centre européen pour les prévisions météorologiques à moyen terme



Series: ECMWF - ESA Contract Report

A full list of ECMWF Publications can be found on our web site under:

<http://www.ecmwf.int/publications/>

© Copyright 2006

European Centre for Medium Range Weather Forecasts
Shinfield Park, Reading, RG2 9AX, England

Literary and scientific copyrights belong to ECMWF and are reserved in all countries. This publication is not to be reprinted or translated in whole or in part without the written permission of the Director. Appropriate non-commercial use will normally be granted under the condition that reference is made to ECMWF.

The information within this publication is given in good faith and considered to be true, but ECMWF accepts no liability for error, omission and for loss or damage arising from its use.

Contract Report to the European Space Agency

**The technical support for global validation of
ERS Wind and Wave Products at ECMWF
(April 2004 - June 2006)**




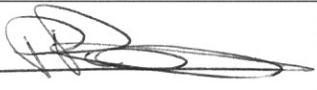
Authors: Saleh Abdalla and Hans Hersbach

Final report for ESA contract 18212/04/I-OL

European Centre for Medium-Range Weather Forecasts

Shinfield Park, Reading, Berkshire, UK

August 2006

	Name	Company	Date	Visa
Prepared by	S. Abdalla	ECMWF	..19/09.../2006	
	H. Hersbach	ECMWF	..19/09.../2006	
Quality Visa	P. Bougeault	ECMWF	..19/09/2006	
Application Authorized by	P. Féménias	ESA/ESRIN	13/08/2006	

Distribution list:**ESA/ESRIN**

Pierre Féménias
Wolfgang Lengert
Pascal Lecomte
Betlem Rosich Tell
ESA ESRIN Documentation Desk

SERCO

Raffaele Crapolicchio
Alessandra Paciucci

ESA/ESTEC

Evert Attema
Paul Snoeij

EUMETSAT

Julia Figa-Saldaña
Hans Bonekamp

ECMWF

HR
Division Section Heads
Lars Isaksen
Ocean Wave Group

Abstract

Contracted by ESA/ESRIN, ECMWF is involved in the global validation and long-term performance monitoring of the wind and wave Fast Delivery products that are retrieved from the Radar Altimeter (RA), the Synthetic Aperture Radar (SAR) and the Active Microwave Instrument (AMI), on-board the ERS spacecraft. Their geophysical content is compared with corresponding parameters from the ECMWF atmospheric and wave model as well as in-situ observations (when possible). Also, tests on internal data consistency are performed.

The project (18212/04/I-OL), which ran from 1 April 2004 to 30 June 2006, is the continuation of previous contracts initiated with ESA/ESRIN and ESTEC. This note presents the final report on the activities performed within the scope of this contract.

An ERS-2 on-board failure in January 2001 degraded attitude control. It had a negative, though acceptable, effect on the quality of the RA and SAR related products; however, a detrimental effect on AMI scatterometer winds. The problems in attitude control were gradually resolved, and since August 2003 the quality of all products is nominal. After 21 June 2003, ERS-2 lost its global coverage permanently due to the failure of both on-board tape recorders. However, the remaining coverage (North Atlantic and western coasts of North America and at a later stage the Southern Ocean and the coasts of East Asia) provides valuable data for assimilation in atmospheric models. Focus of this report will be on that period.

Furthermore, an overview evaluation of the wind and wave products from the entire ERS mission is carried out. The products involved are the fast delivery AMI scatterometer wind and SAR wave mode spectra and the off-line ocean product (OPR) wind and wave data from both ERS-1 and ERS-2 missions.

1 Introduction

The ERS mission is a great opportunity for the meteorological and ocean-wave communities. The wind and wave products from ERS-1/2 provide an invaluable data set. They form some kind of benchmarks against which model products can be validated. In addition, they are assimilated in the models to improve the predictions. On the other hand, consistent model products, especially first-guess products, can be used to validate and monitor the performance of the satellite products.

The European Centre for Medium-Range Weather Forecasts (ECMWF) has been collaborating with the European Space Agency (ESA) since the beginning of the ERS-1 mission in performing the global validation and long-term performance monitoring of the wind and wave products. These products are retrieved from three instruments, defining three Fast Delivery (FD) products that are received at ECMWF in BUFR format. Significant wave height and surface wind speed (URA product) are obtained from the Radar Altimeter (RA). Ocean image spectra (UWA product) are from the Synthetic Aperture Radar (SAR). Surface wind speed and direction (UWI product), finally, are retrieved from the Active Microwave Instrument (AMI) scatterometer. In-house developed monitoring tools are used for the comparison of these products with corresponding parameters from the ECMWF atmospheric (IFS) and wave (ECWAM) models (IFS Documentation, 2004). Whenever possible, these tools include a comparison with in-situ measurements. In addition, tests are performed on the internal consistency of the underlying observed quantities measured by the three instruments.

This support has been carried out within the framework of several consecutive contracts with ESA. The current contract (18212/04/I-OL), which is supervised by the European Space Research Institute (ESRIN), ran from 1 April 2004 to 30 June 2006. Findings from the monitoring activities described above are summarized in monthly or cyclic (depending on the product) data quality and validation reports. These reports are sent regularly to ESRIN. Besides giving an overview on instrument performance and scientific interpretation, these

reports also include recommendations to ESA for refinements of calibrations, further algorithm development and model tuning. Such recommendations are based on a long-term analysis of the relevant parameters.

In addition to these monitoring activities, dedicated studies on data quality and related scientific research have been carried out. These embrace, among others, collocation studies, algorithm development and the incorporation of ERS wind and wave data in the operational ECMWF assimilation system. As a result, ERS altimeter wave heights have been assimilated in the ECMWF wave model since 15 August 1993 (Janssen *et al.* 1997). It was replaced by ENVISAT Radar Altimeter-2 (RA-2) on 22 October 2003. Scatterometer winds were introduced in the atmospheric variational assimilation system on 30 January 1996 (for a description of its impact, see Isaksen and Janssen 2004). It was re-introduced on 8 March 2004 (Hersbach *et al.* , 2004a), after the suspension in January 2001. The assimilation of SAR wave mode spectra in the ECMWF wave model, on the other hand, was realised on 13 January 2003. ERS-2 SAR assimilation was replaced by ENVISAT Advanced Synthetic Aperture Radar (ASAR) Level 1b wave mode spectra on 1 February 2006.

This document presents the final report of the present contract. It provides a focus on the performance of the wind and wave products over a period of about three years.

Since the ERS mission is approaching the end of its lifetime, it is thought opportune to make a review of the quality of the various products from both ERS-1 and ERS-2 satellites. Those products are the fast delivery (FD) scatterometer wind (UWI) product, FD SAR Wave Mode (UWA) product and both FD (URA) and the off-line OPR (Ocean Product) altimeter wind and wave products.

In Section 2, the performance of altimeter FD URA data in the North Atlantic will be considered. Section 3 presents the global performance of the altimeter OPR product for the whole lifetime of the ERS mission. An overview of the performance of the SAR significant wave height, both globally and in the North Atlantic, will be presented in Section 4, and of UWI wind data in Section 5. In Section 6, conclusions are formulated, and the report ends with a list of ECMWF model changes since November 2000.

Acronyms

AMI	Active Microwave Instrument
ASPS	Advanced Scatterometer Processing System
AOCS	Attitude and Orbit Control System
ASAR	Advanced Synthetic Aperture Radar
ASCAT	Advanced SCATterometer
ASCII	American Standard Code for Information Interchange
BUFR	Binary Universal Form for the Representation of meteorological data
CERSAT	French ERS Processing and Archiving Facility (Centre ERS d'Archivage et de Traitement)
CMEDS	Canadian Marine Environmental Data Service
CMOD	C-band Geophysical MODEL function
EBM	Extra Back-up Mode
ECMWF	European Centre for Medium-range Weather Forecasts
ECWAM	ECMWF Wave Model (an enhanced version of WAM model)
ENVISAT	ENVIronmental SATellite
ERA-40	ECMWF 40-Year Reanalysis
ERS	European Remote sensing Satellite
ESA	European Space Agency
ESACA	ERS Scatterometer Attitude Corrected Algorithm
ESTEC	European Space research and TEchnology Centre
ESRIN	European Space Research INstitute
FD	Fast Delivery product
FEEDBACK	data to which information on usage in the ECMWF assimilation system has been added
FG	ECMWF First Guess with a time resolution of 3 hours
FGAT	First Guess at Appropriate Time
GMF	scatterometer Geophysical Model Function
GTS	Global Telecommunication System
HRES	High RESolution
IDL	Interactive Data Language
IFREMER	French Research Institute for Exploitation of the Sea (Institut français de recherche pour l'exploitation de la mer)
IFS	Integrated Forecast System
JPL	Jet Propulsion Laboratory
KNMI	Koninklijk Nederlands Meteorologisch Instituut
LRDPF	Low Rate Data Processing Facility
LBR	Low Bit Rate
MPI	Max-Planck-Institut for meteorology, Hamburg
NESDIS	National Environmental Satellite Data and Information Service
NDBC	U.S. National Data Buoy Center
NH	Northern Hemisphere
NRES	Nominal RESolution
NRT	Near-Real Time
NSCAT	NASA (National Aeronautics and Space Agency) Scatterometer
OPR	(ERS Radar Altimeter) Ocean PProduct



QC	Quality Control
QSCAT	QuikSCAT (Quick Scatterometer)
RA	Radar Altimeter
RA-2	(ENVISAT) Radar Altimeter-2
RMSE	Root-Mean Square Error
SAR	Synthetic Aperture Radar
SH	Southern Hemisphere
SI	Scatter Index
STDV	STandard DeViation (of the Difference)
SWH	Significant Wave Height
TAO	Tropical Atmosphere Ocean project
UKMO	UK Met Office
URA	User FD Radar Altimeter product
UTC	Coordinated Universal Time
UWA	User FD SAR WAve product
UWI	User FD scatterometer WInd product
WAM	third-generation ocean-WAve Model
WMO	World Meteorological Organization
ZGM	Zero-Gyro Mode

2 The Radar Altimeter URA Product

Each URA (User fast delivery Radar Altimeter) product is sampled at 7 km along the satellite ground track. First the altimeter data stream is divided into sequences of 30 individual neighbouring observations. Erroneous and suspicious individual observations are removed and the remaining data in each sequence are averaged to form a representative super-observation, provided that the sequence has at least 20 "good" individual observations. Then, further monitoring is performed with respect to these super-observations, which, for this purpose are collocated with ECMWF model parameters and buoy data. Focus is on URA backscatter, URA wind speed and URA significant wave height.

2.1 Data Coverage after June 2003

The loss of the global coverage due to the failure of the on-board low-bit rate tape recorders in June 2003 reduced the number of observations received at ECMWF to about 13% of the full coverage data volume as can be seen in Figure 1 which shows the daily rate of total number of the altimeter super-observations processed at ECMWF. Assessment of the long-term quality of the product after the loss of the global coverage can not be done by comparing it with statistics when there was full coverage. For practical reasons it is not easy to re-process the product over a rather long period for the exact area under current coverage. Instead, readily available long-term statistics for the closest region is considered for comparison. The region covering the extra-tropical Northern Atlantic (north of latitude 20°N) is used as a common area with almost complete coverage before and after the loss of the global coverage. The 7-day running average of daily number of altimeter super-observations in the North Atlantic since the beginning of year 2000 is shown in Figure 2. It is clear that the current coverage in the North Atlantic is slightly lower than the usual coverage. The missing coverage is towards the southern edge of the region as can be seen in Figure 3. For the URA product, we will focus our attention on the quality of the altimeter products for the current coverage or specifically in the North Atlantic.

2.2 Monitoring of URA Significant Wave Height in the North Atlantic

As usual, URA significant wave heights (SWH) are rather stable and of good quality, apart from the overestimation of small SWH values. Figure 4 shows the time history of the daily bias between the altimeter and the ECMWF operational model wave heights in the North Atlantic since the beginning of year 2000. After excluding the apparent anomalous altimeter behaviour during March-April 2000 and February 2001 one can distinguish a seasonal cycle of bias in Figure 4 with a minimum value taking place around April-May and a maximum value occurring around October-November before the loss of the global coverage. This seasonal cycle became stronger after the loss of the global coverage with the minimum and maximum values shifted earlier by about one month. Although it is difficult to pinpoint the reason for the stronger cycle, recent model changes like the unresolved bathymetry treatment introduced on 9 March 2004 and the change of wave model dissipation introduced on 5 April 2005 are possible candidates. Another possible reason could be related to the uncovered part towards the southern edge of the area (see Figure 3) which shows less variability than the higher latitudes. Figure 4 displays a clear general trend of reduced bias over the years as well. This is mainly due to the model improvements. Recently, the bias seems to fluctuate around the zero value. Apart from that, the bias between the altimeter and the model wave heights did not suffer any abrupt changes after the loss of the global coverage.

Figure 5 shows the time history of the daily scatter index (SI) of the altimeter significant wave height with respect to the ECMWF wave model (ECWAM) in the North Atlantic since the beginning of year 2000. Both the seasonal variation (maximum during July-August and minimum during December-January) and the general

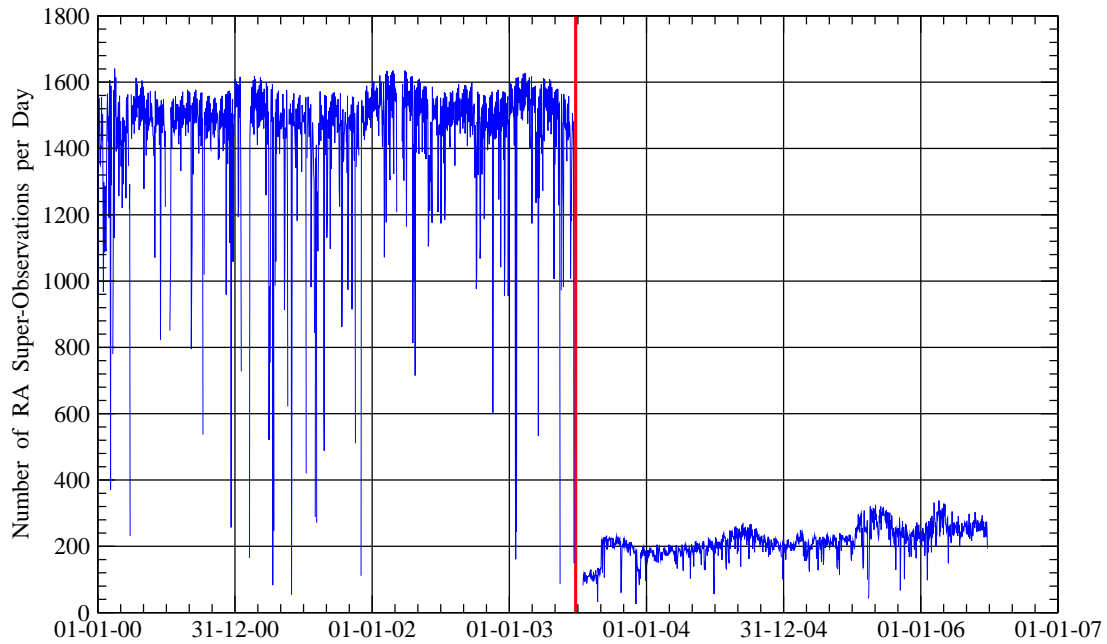


Figure 1: Time history of the total number of ERS-2 altimeter super-observations processed at ECMWF per day since 1 January 2000. Date of loss of global coverage is represented by a red thick vertical line.

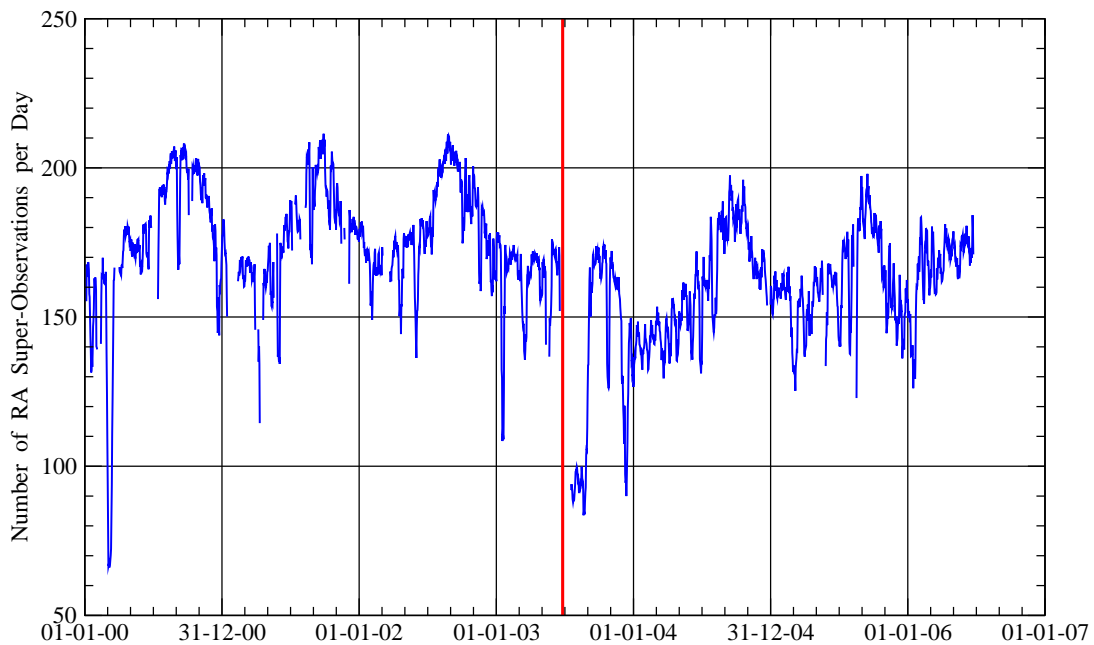


Figure 2: Time history of the 7-day running average of daily number of altimeter super-observations in the North Atlantic since 1 January 2000. Date of loss of global coverage is represented by a red thick vertical line.

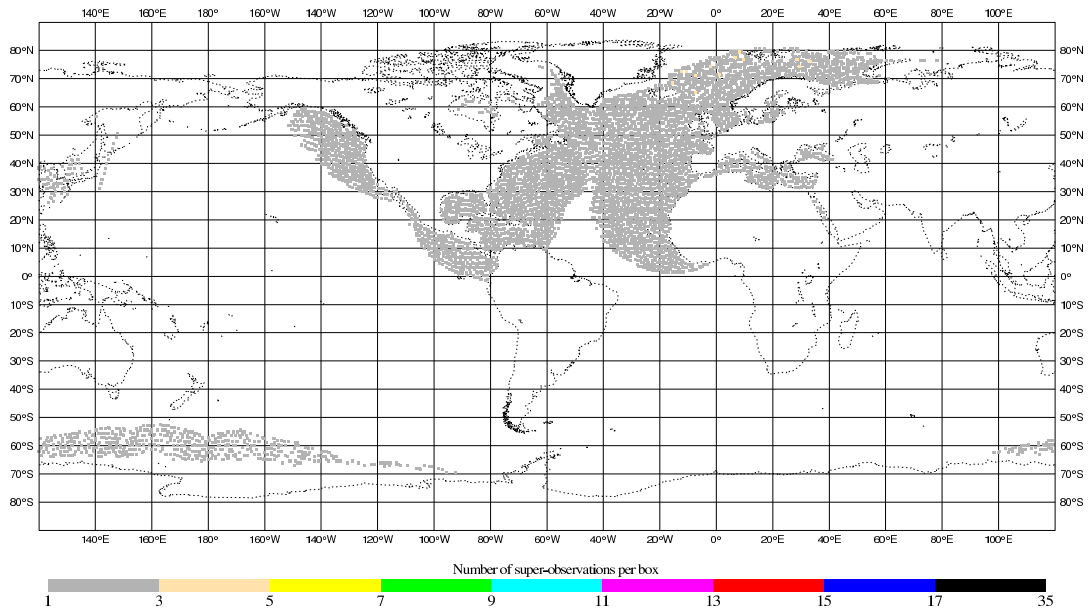


Figure 3: Typical recent ERS-2 radar altimeter monthly coverage (June 2006).

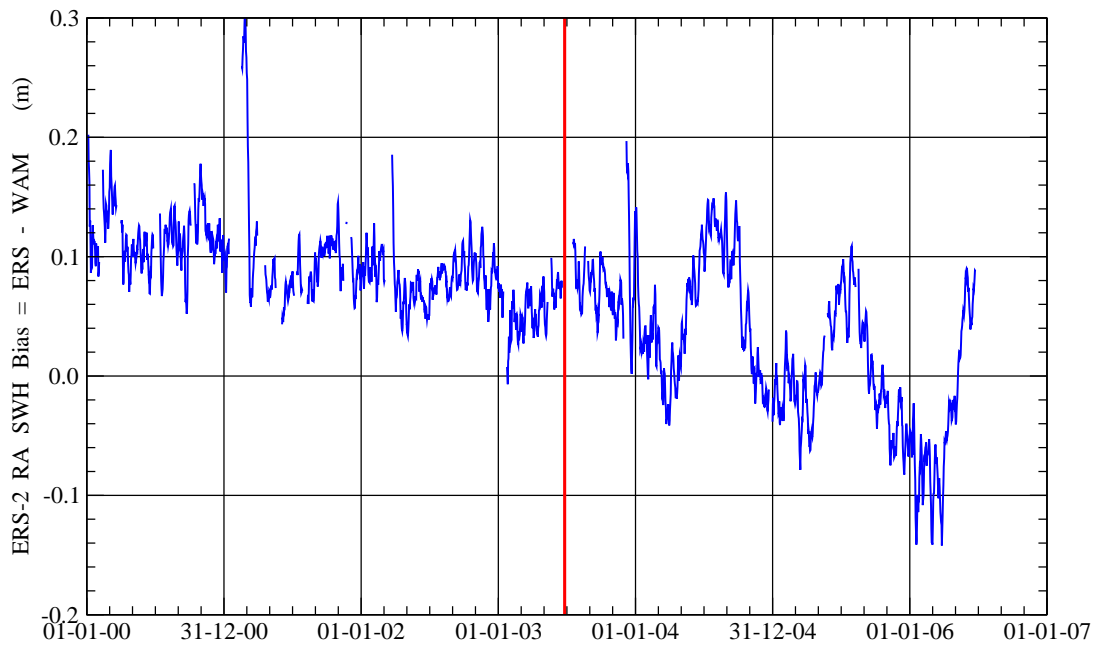


Figure 4: Time history of the 7-day running average of daily bias of altimeter significant wave height with respect to wave model in the North Atlantic since 1 January 2000. Date of loss of global coverage is represented by a red thick vertical line.

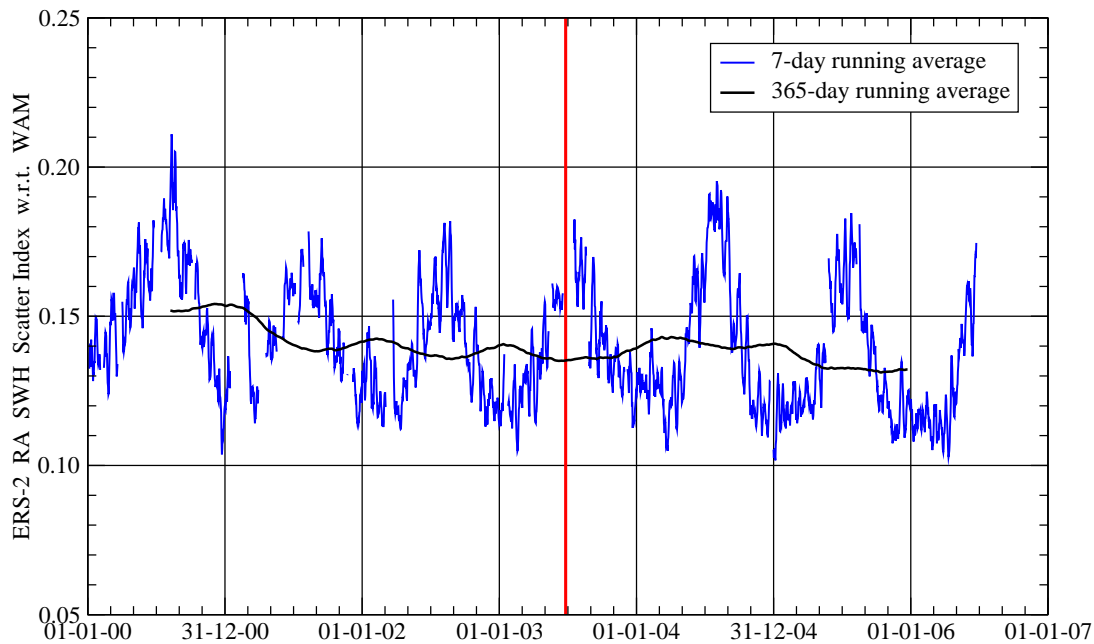


Figure 5: Time history of the 7-day running average of daily scatter index of altimeter significant wave height with respect to wave model in the North Atlantic since 1 January 2000. The thick black line shows the SI trend (365-day running average). Date of loss of global coverage is represented by a red thick vertical line.

trend of the reduction in SI (the 365-day running average) can be seen. Again the seasonal variation seems to be stronger after the loss of global coverage. The higher SI values during July and August 2004 are due to a technical problem that prevented the ENVISAT RA-2 SWH product from being assimilated in the wave model.

In summary, it is possible to say that the altimeter significant wave height product is as good as it used to be. Other statistics (not shown) deliver the same message. It is worth mentioning that the ERS-2 altimeter wave height product was assimilated in the ECMWF wave model until it was replaced by the corresponding product from ENVISAT on 21 October 2003.

2.3 Monitoring of URA Surface Wind Speed in the North Atlantic

Before the loss of the global coverage, URA wind speed observations were not as good as the wave heights. They suffered several periods of degraded quality, especially after the start of the problems with the on-board gyros early 2000 as will be described later in Section 3.4. The "sun blinding effect" is responsible for most of the degradation in the Southern Hemisphere (SH) during the period between mid-January to early March each year since year 2000.

Figure 6 shows the time history of the daily bias of URA surface wind speed with respect to the ECMWF operational atmospheric model in the North Atlantic since 1 January 2000. The wind speed bias in the North Atlantic follows a seasonal cycle with positive bias (maximum) in the Northern Hemispheric (NH) winter and negative (minimum) in the NH summer can be clearly seen. Since early 2001, this seasonal cycle started to be symmetric around the zero line. This can be attributed to the ECMWF high-resolution model T511 implemented on 20 November 2000. The same behaviour continued after the loss of the global coverage. On the other hand, Figure 7 shows the time history of the daily SI of surface wind speed with respect to the

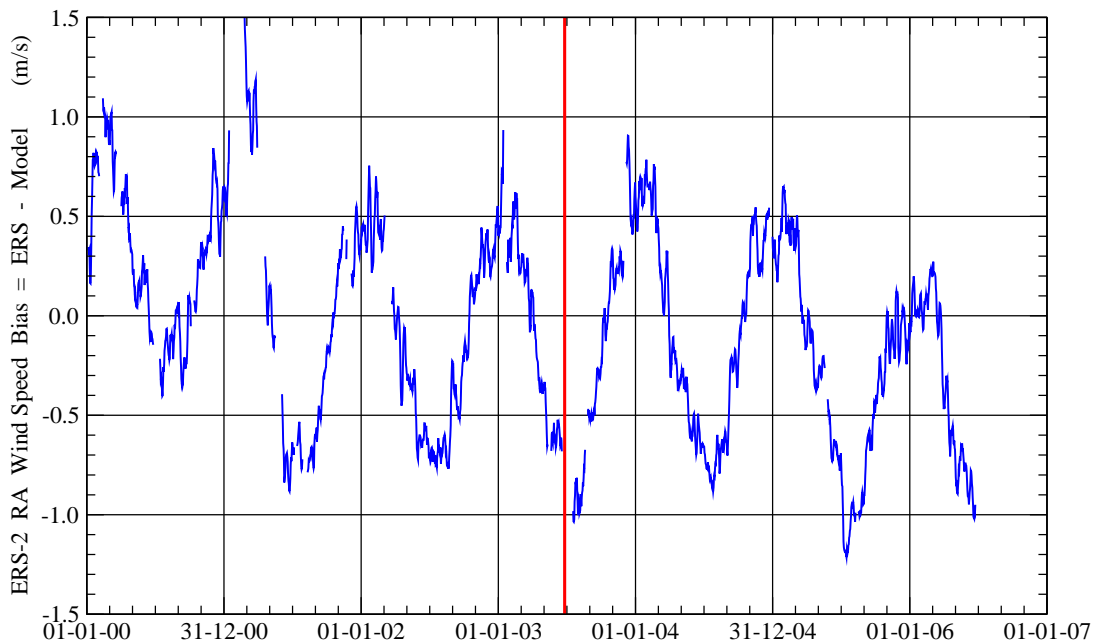


Figure 6: Time history of the 7-day running average of daily bias of altimeter surface wind speed with respect to the ECMWF atmospheric model in the North Atlantic since 1 January 2000. Date of loss of global coverage is represented by a red thick vertical line.

ECMWF operational atmospheric model in the North Atlantic since 1 January 2000. The SI follows a seasonal cycle with low values occurring during the NH winter and vice versa in summer. The exception to this cycle is the period from early January to early March each year since 2001. This may be due the residual effect of the "sun blinding effect". Continuous improvements of the ECMWF operational atmospheric model result in lower wind speed scatter index values between this model and the altimeter. A drop in SI early 2002 can be clearly recognised. This coincides with a model change including the assimilation of QuikSCAT wind speeds. The usual trend of the SI reduction continued after the reduction of ERS-2 coverage. The only exception is the relatively higher scatter index during January and February 2004.

2.4 Monitoring of URA Altimeter Backscatter

Altimeter backscatter is the raw observation that is translated into surface wind speed. Figure 8 displays the long-term monthly global mean backscatter coefficient values since December 1996. Before the loss of the global coverage, the monthly mean value used to be around 11.0 dB. However, the mean values used to increase to more than 11.4 dB for the month of July in years 1997 to 1999. Those peaks disappeared in year 2000 and later. Instead, the mean backscatter coefficient started to be rather low in the month of February (or March) each year from 2000. This is a direct result from the sun blinding effect.

After the loss of the global coverage, the monthly mean started to have a strong seasonal cycle varies between 10.4 and 12.2 dB. This cycle has a peak during the NH summer (July-August) and a trough during winter (December-January). This is an expected behaviour in the NH. After the extension of the ERS-2 coverage by including more ground stations especially in the SH, the amplitude of the seasonal cycle of mean backscatter coefficient started to get smaller. The impact of including McMurdo and Hobart ground stations can not be missed in Figure 8.

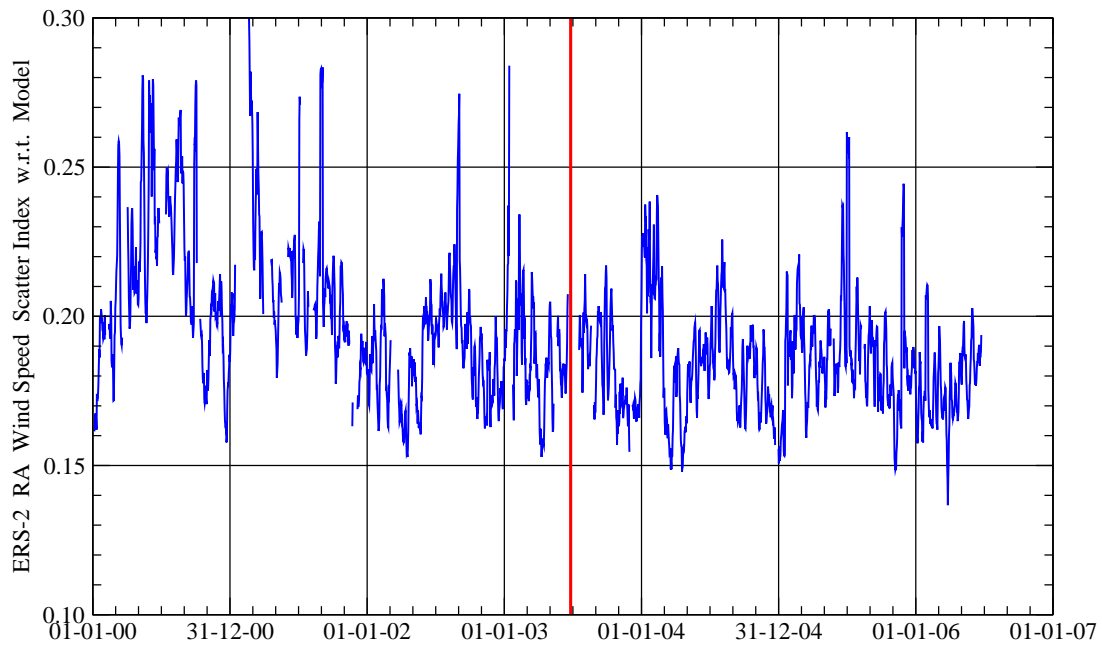


Figure 7: Time history of the 7-day running average of daily scatter index of altimeter surface wind speed with respect to the ECMWF atmospheric model in the North Atlantic since 1 January 2000. Date of loss of global coverage is represented by a red thick vertical line.

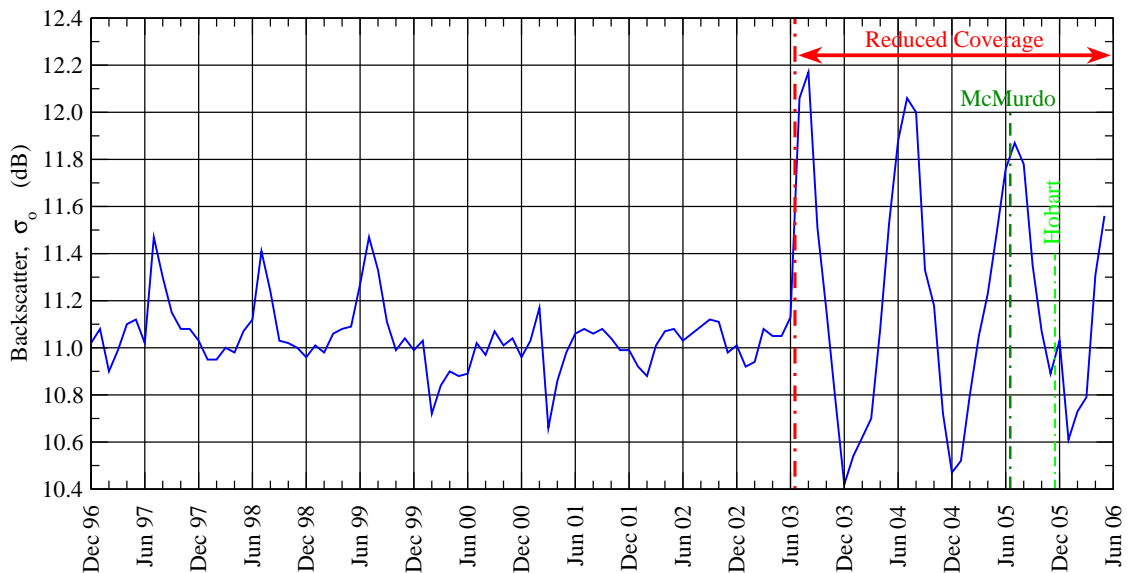


Figure 8: Time history of the monthly global mean of ERS-2 altimeter backscatter coefficient after QC since December 1996.

3 The Radar Altimeter OPR Product

3.1 Introduction

The ERS missions started with the launch of ERS-1 (the first sun-synchronous polar-orbiting mission of ESA) on 17 July 1991. It was followed by ERS-2 which was launched on 21 April 1995. The Radar Altimeter (RA) and the Active Microwave Instrument (AMI) which consists of two separate radars; namely: the Synthetic-Aperture Radar (SAR) and the Scatterometer, are the instruments which are able to provide wind and wave data on-board both satellites.

According to ESA (2005), the launch and early orbit phase (LEOP) of ERS-1 began with the launch and ended with the satellite achieving nominal attitude and orbit. The duration of this initial phase was less than two weeks. A 3-day repeat cycle was adopted to provide frequent revisits to a number of dedicated sites for calibration purposes. The remaining effective life of the ERS-1 mission is sub-divided into the following phases:

- **Phase A - Commissioning Phase:** 3-day repeat cycle. Lasted 138 days (from 25 July to 10 December 1991). Mainly to perform engineering calibration and geophysical validation.
- **Phase B - First Ice Phase:** 3-day repeat cycle. Lasted 93 days (from 28 December 1991 to 31 March 1992). Optimised for the specific requirements of Arctic ice experiments.
- **Phase R - Experimental Roll Tilt Mode Campaign:** 35-day repeat cycle. Lasted 12 days (from 2 to 14 April 1992). The satellite body was rotated by 9.5 degrees allowing operation of the SAR imaging mode at an incidence angle of 35 degrees. Performance of the RA Altimeter is slightly degraded because of the geocentric pointing instead of the local normal pointing.
- **Phase C - Multi-Disciplinary Phase:** 35-day repeat cycle. Lasted 20 months (14 April 1992 to 23 December 1993). Mean sea surface determination, ocean variability studies and surface mappings are among various uses during this phase.
- **Phase D - Second Ice Phase:** 3-day repeat cycle similar to the First Ice Phase (Phase B). Lasted 108 days (from 23 December 1993 to 10 April 1994).
- **Phase E - Geodetic Phase:** 168-day repeat cycle. Lasted about 5 months (from 10 April 1994 to 28 September 1994). Enables high-density measurements to improve the determination of the geode using RA.
- **Phase F - Shifted Geodetic Phase:** 168-day repeat cycle similar to the Geodetic Phase (Phase E) but with an 8 km spatial shift. Lasted about 6 months (from 28 September 1994 to 21 March 1995).
- **Phase G - Second Multi-Disciplinary Phase:** 35-day repeat cycle similar to the first Multi-Disciplinary Phase (Phase C). Lasted about 14 months (from 21 March 1995 to 2 June 1996). Tandem mission with ERS-2 (from 17 August 1995 to 2 June 1996) was within this phase.

Phase G concluded the nominal ERS-1 mission. ERS-1 stayed in this configuration while serving as a back up for ERS-2. ERS-1 finally retired on 10 March 2000 after a failure in its on-board attitude control system.

On the other hand, ERS-2 had only two phases of operations both with the same orbital configuration of 35-day repeat cycle:

- **Phase A - Commissioning Phase:** Lasted from 2 May 1995 to 17 August 1995. Mainly to perform engineering calibration and geophysical validation.
- **Phase B - Routine Phase:** Started on 17 August 1995 and still going on. Similar to ERS-1 Phases C and G. This phase started with the tandem mission from 17 August 1995 to 2 June 1996.

ERS-2 was unfortunate to start losing its gyroscopes in early 2000. This led to the implementation of the Attitude and Orbit Control System (AOCS) mono-gyro attitude software early February 2000 (c.f. Féménias and Martini, 2000). Further loss of gyroscopes on 17 January 2001, which left a single working gyroscope, forced the piloting of the spacecraft without any gyroscopes in the Extra Back-up Mode (EBM). This led to degradation of some ERS-2 products. The implementation of the zero-gyro mode (ZGM) was introduced in June 2001 to assist the piloting of the spacecraft without any need for the frequent use of the only available gyroscope.

Finally, the permanent failure of the ERS-2 low bit rate (LBR) tape recorders on 21 June 2003 prevented the continuation of the ERS-2 global coverage. ERS-2 LBR data coverage is limited within the vicinity of the ground stations. The recent coverage map is shown in Figure 3.

3.2 Data Sources and Collocations

ERS altimeter OPR data products were obtained from the French ERS Processing and Archiving Facility (CER-SAT) of the French Research Institute for Exploitation of the Sea (IFREMER). The data were converted into BUFR format. The same operational pre-processing and quality control procedures (c.f. Abdalla and Hersbach, 2004) were applied before the use of the data. The only exception is that the number of 1-Hz observations averaged to produce one super-observation was selected to be 11 (rather than the value of 30 used operationally for ERS-2).

As both operational atmospheric and wave models at ECMWF are changing frequently, the operational ECMWF data archive does not represent a consistent data set to be used for the evaluation of the ERS products. The quality of both wind and wave fields are improving with time. Since we are after a long-term evaluation of ERS products, a more consistent data set (free of other changes) is needed. Therefore, it was found appropriate to use the ECMWF 40-Year Reanalysis (ERA-40) wind fields for the validation. ERA-40 fields were produced using the same atmospheric model for the entire period of the reanalysis from September 1957 to August 2002. The model used in the reanalysis has a spectral resolution of T159 (c.f. Uppala et al., 2005) which corresponds to about 125 km. Although this is much coarser than the operational resolution during the last few years, ERA-40 resolution is much higher than the operational resolutions at earlier times. Furthermore, ERA-40 represents a rather consistent data set as far as the model is concerned. The amount and quality of the observations assimilated in ERA-40 varied by time during the ERA-40 period. This, of course, has some (hopefully minor) impact on the consistency of ERA-40 products. However, in the absence of another alternative, one can make use of this data set.

The wave model used in ERA-40 was of rather coarser resolution (1.5 degree which is about 156 km). Although this may not be a major concern in the open ocean, it has a definite detrimental impact on wave fields in the inner seas and near the coasts. Therefore, we decided not to use ERA-40 wave fields for the evaluation of ERS OPR wave products. Instead a long term stand-alone wave model hindcast run (without any data assimilation) was used. The model used for this run is the latest version of the ECMWF wave model (ECWAM) which includes several enhancements, both physics and numerics, over the standard WAM model (c.f. Janssen, 2004, Janssen et al., 2005 and Bidlot et al., 2006). The model resolution is 0.5 degrees (about 55 km). ERA-40 wind fields were used to force the model.

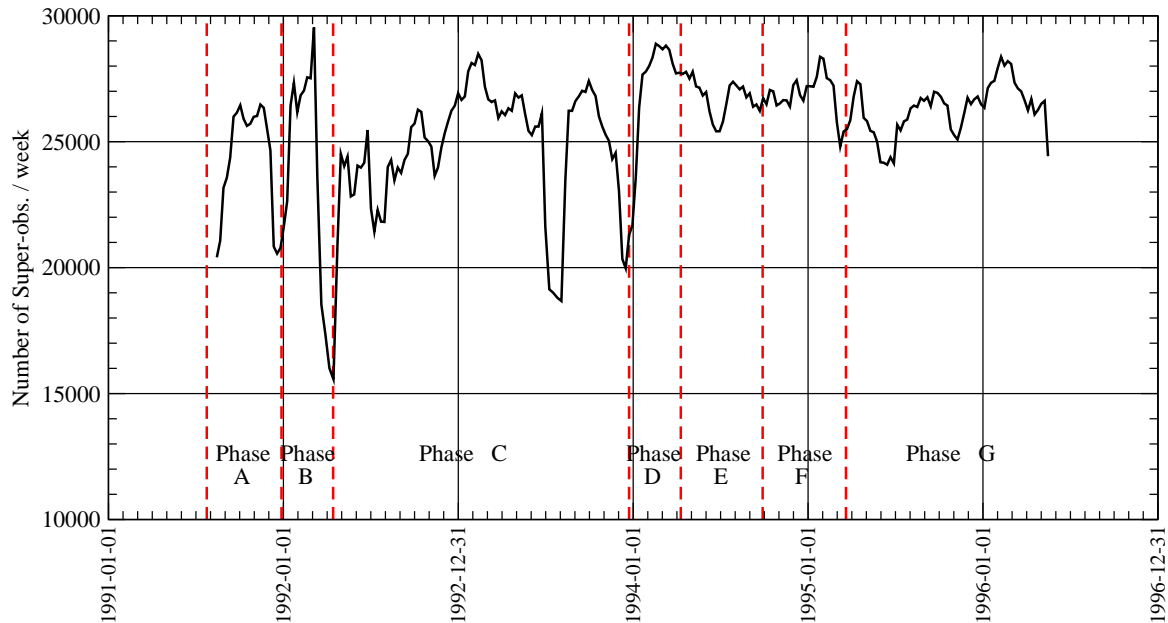


Figure 9: Time history of the 5-week running average of weekly number of ERS-1 altimeter super-observations during the effective lifetime of ERS-1 (August 1991 to May 1996). Various ERS-1 phases are displayed.

The ERA-40 data set covers the period until 31 August 2002. After that date, operational wind fields were used for ERS-2 wind speed products. The same wind fields were used to force the wave model beyond ERA-40 period. It is important to note that the operational wind fields are of much better quality than ERA-40 due to the recent model enhancements and to the higher resolution. Naturally one should expect better wave fields as a result of using such wind fields for the hindcast run.

The radar altimeter super-observations were collocated with the corresponding model counterparts. Each week worth of collocations are used to compute various statistics. The time histories of those statistics are examined to draw conclusions related to the altimeter wind and wave products. To concentrate on long-term changes it was necessary to filter out the short term variability (noise) of those plots by using 5-weekly running averages.

3.3 ERS-1 Altimeter OPR Product

Figure 9 shows the time history of the weekly number of super-observations of ERS-1 altimeter OPR products during the effective lifetime of ERS-1 (August 1991 to May 1996). Note that the number of 1-Hz observations averaged to form each super-observation is 11. This is the reason for the higher number of super-observations compared to the operational plots of URA product (e.g. ERS-2 URA plot of Figure 1).

Figure 10 shows the time history of the weekly bias of ERS-1 altimeter significant wave height with respect to the ECWAM model hindcast (using ERA-40 reanalysis wind fields) during the effective lifetime of ERS-1. Both (absolute) bias and bias relative to the model mean (relative bias) are shown. It is clear that ERS-1 OPR SWH is in general lower than the model by about 18 cm (about 7%). The seasonal cycle of the bias can not be missed. Normalising with the mean model wave height does not totally eliminate this seasonal cycle. The underestimation of ERS-1 SWH with respect to the model varies between about 12 cm (during the NH summer) and about 24 cm (in NH winter). This corresponds to about 5% and 11%, respectively. It is worthwhile mentioning that during the first two months of the ERS-1 mission (August-September 1991), the

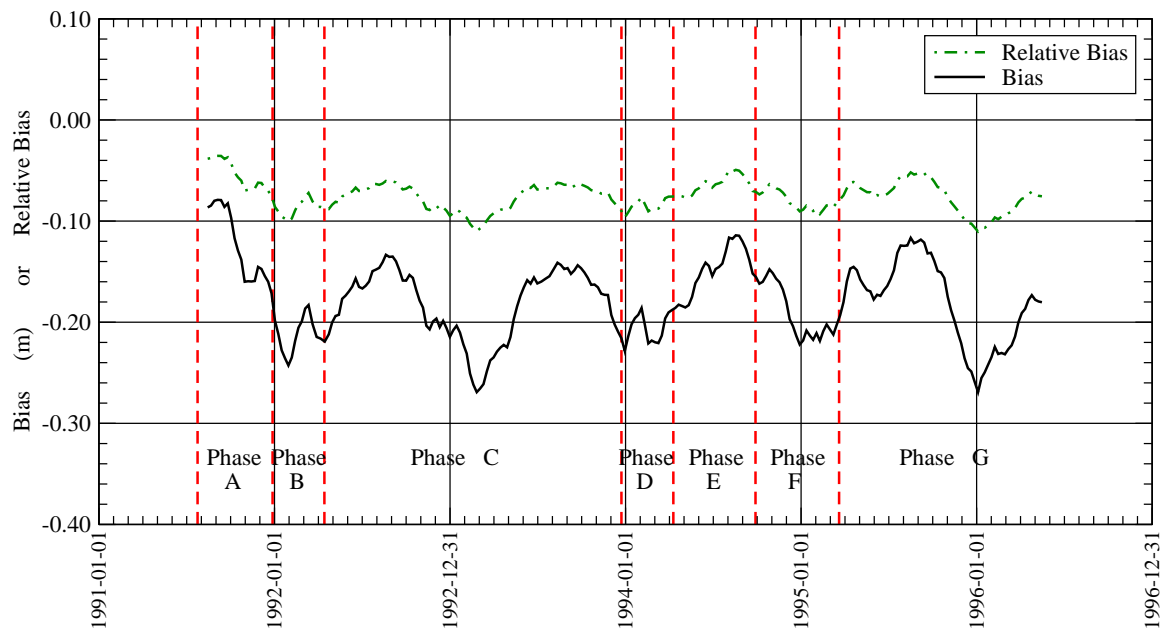


Figure 10: Time history of the 5-week running average of weekly global bias and relative bias (i.e. the bias normalised by the model mean) of ERS-1 altimeter significant wave height with respect to the ECWAM model hindcast (using ECMWF ERA-40 reanalysis wind fields) during the effective lifetime of ERS-1 (August 1991 to May 1996). Various ERS-1 phases are displayed.

SWH bias was the smallest ever during the entire mission. It seems that the various ERS-1 phases do not have any impact on SWH bias.

The time history of the weekly SI of ERS-1 OPR SWH with respect to the same wave model hindcast during the whole effective lifetime of ERS-1 is shown in Figure 11. The SI fluctuated around a mean value of about 16% with a seasonal cycle especially for the period starting from early 1993. Before that the SI was fluctuating at a higher level of about 17%. Unlike the SWH bias, SI was the highest during the first two months of the mission. Again, there is no clear evidence on any impact of orbit configuration changes (phases) on the SWH SI.

Figure 12 shows the time history of the weekly bias of ERS-1 altimeter surface wind speed with respect to ERA-40 wind fields during the entire effective lifetime of ERS-1 (August 1991 to May 1996). It is clear that the ERS-1 lifetime can be divided into four main distinct periods in terms of wind speed bias characteristics. The limits of each period coincide with ERS-1 orbital configuration changes (phases). During the Commissioning (Phase A) and the First Ice (Phase B) phases, which share the same orbital configurations of 3-day repeat cycle, the wind speed bias was around -0.10 m s^{-1} . The start of the Multi-Disciplinary Phase (Phase C), which has a 35-day repeat cycle, coincides with a jump in the wind speed bias to about $+0.40 \text{ m s}^{-1}$. Within the above two periods, there is a linear increase in the wind speed bias. A bias drop occurred at the beginning of the Second Ice Phase (D), which has a 3-day repeat cycle, to about $+0.07 \text{ m s}^{-1}$. The same bias continued until the end of the Shifted Geodetic Phase (F), when the repeat cycle was 168 days. One can even notice a slight change in bias (drop to about $+0.13 \text{ m s}^{-1}$) in the transition from Phase E to Phase F. Finally, with the start of the 35-day repeat-cycle Phase G (Second Multi-Disciplinary), the wind speed bias jumped to about $+0.50 \text{ m s}^{-1}$. Even within Phase G, there is also a systematic trend in the bias.

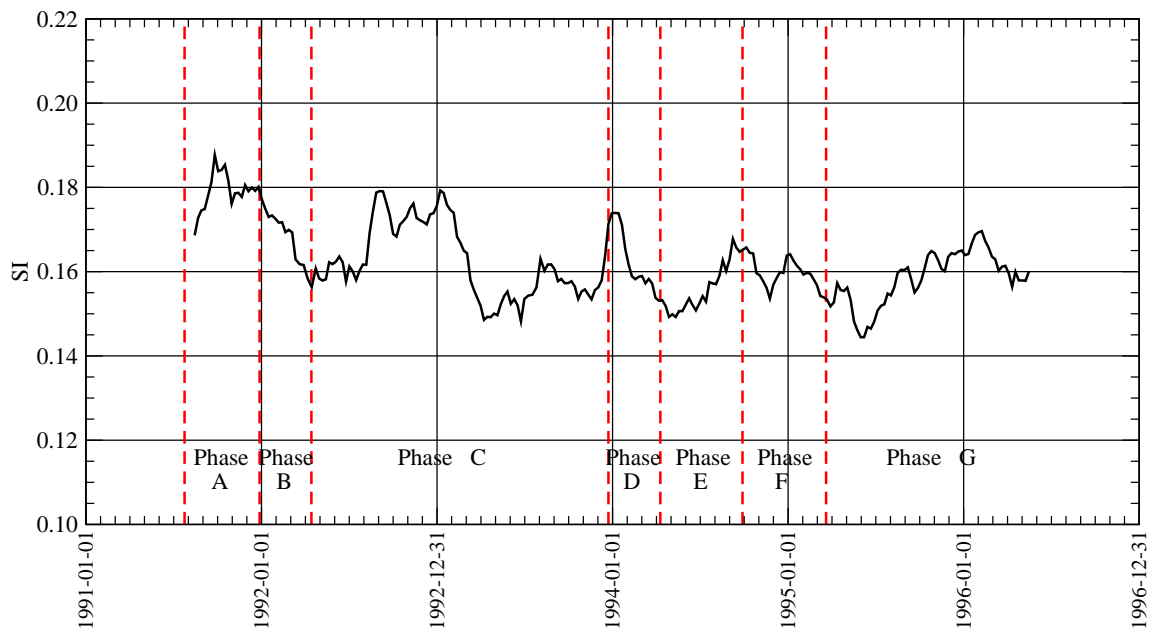


Figure 11: Time history of the 5-week running average of weekly global scatter index of ERS-1 altimeter significant wave height with respect to the ECWAM model hindcast (using ECMWF ERA-40 reanalysis wind fields) during the effective lifetime of ERS-1 (August 1991 to May 1996). Various ERS-1 phases are displayed.

The above correlation may suggest some dependency of the wind speed bias on the orbit configuration. However, it is difficult to explain the different bias levels between Phases B and D which have same repeat cycle of 3 days and between Phases E and F which have repeat cycles of 168 days. Furthermore, Phases D and E have different repeat cycles (3 for the former and 168 for the latter) but have the same level of bias.

The use of a rather consistent model wind data set (ERA-40) reduces the responsibility of the model for the abrupt changes in wind speed bias. Furthermore, the coincidence of the wind speed bias jumps with the change of ERS-1 phases, make us confident that the problem lies in the ERS-1 OPR wind speed product.

Figure 13 displays the long-term 5 week running average of weekly global mean backscatter coefficient values over the effective lifetime of ERS-1. The mean backscatter coefficient is slightly below 11 dB. It is possible to distinguish periods similar to those described in the wind speed bias (Figure 12). This confirms that the changes of wind speed bias are due to the changes in the altimeter instrument or the processing algorithms to provide the backscatter coefficients.

The time history of the weekly SI of the ERS-1 OPR surface wind speed with respect to ERA-40 is shown in Figure 14. During the Commissioning Phase, the wind speed SI was relatively high and reached about 25%. With the start of Phase B (the First Ice Phase), the SI reduced considerably to about 22%. During Phases B and C, there seems to be a seasonal cycle with high SI during the NH winter and low values during the summer. This cycle was interrupted with local peaks at the start of each phase. During the Second Multi-Disciplinary Phase the wind speed SI was stabilised at a level slightly below 22%.

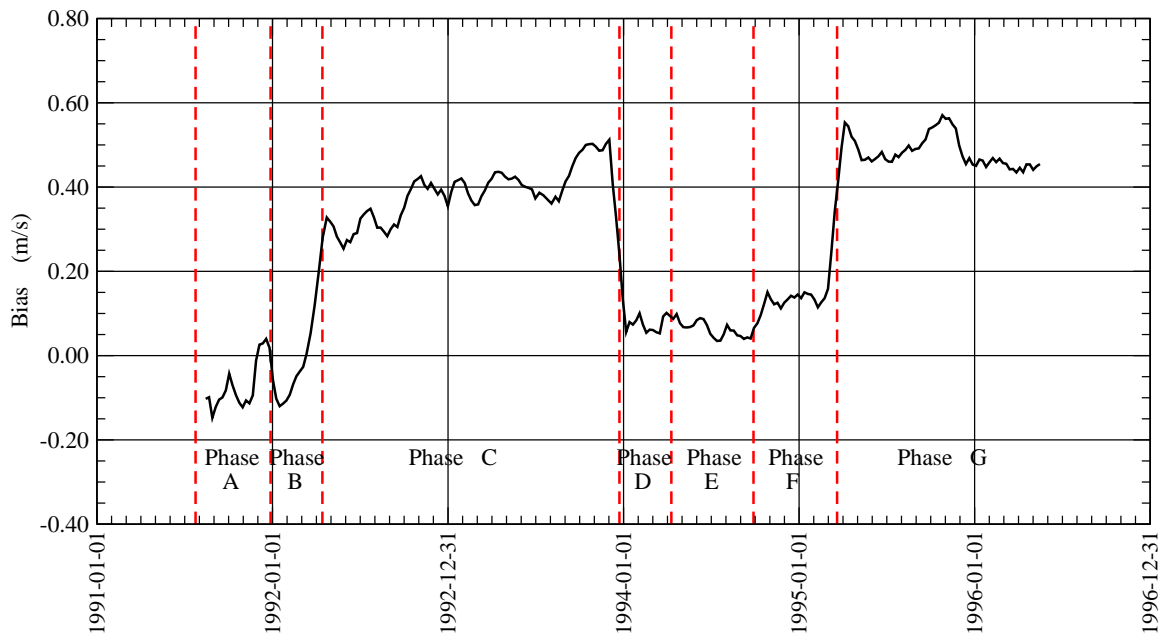


Figure 12: Time history of the 5-week running average of weekly global bias of ERS-1 altimeter surface wind speed with respect to the ECMWF ERA-40 re-analysis during the effective lifetime of ERS-1 (August 1991 to May 1996). Various ERS-1 phases are displayed.

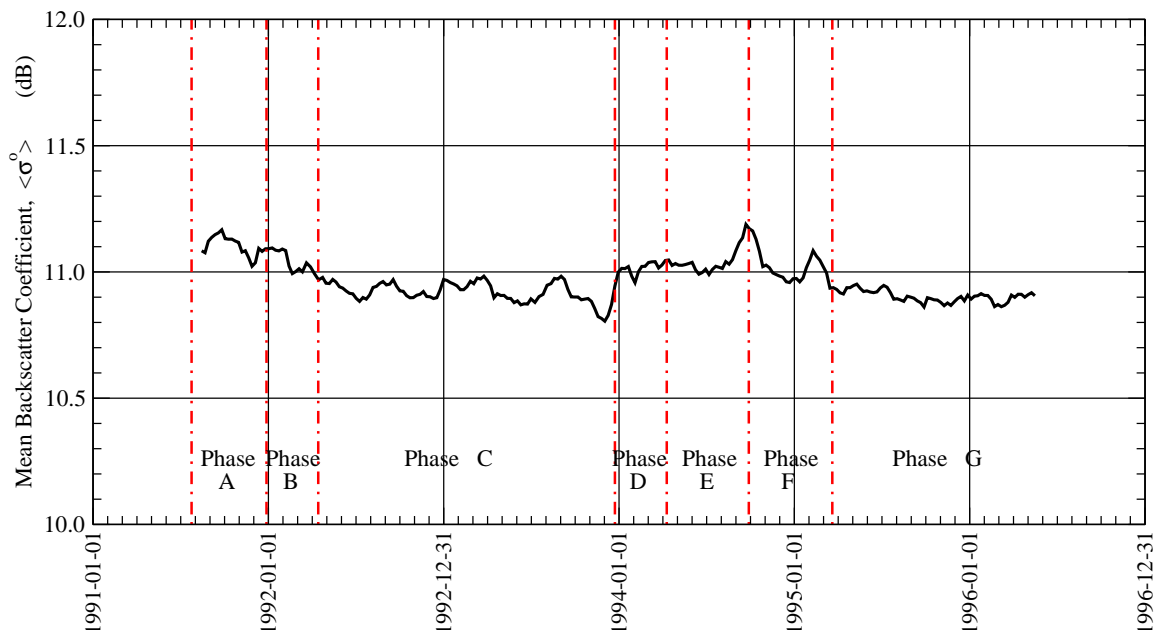


Figure 13: Time history of the 5-week running average of weekly global mean ERS-1 altimeter backscatter coefficient after QC during the effective lifetime of ERS-1 (August 1991 to May 1996). Various ERS-1 phases are displayed.

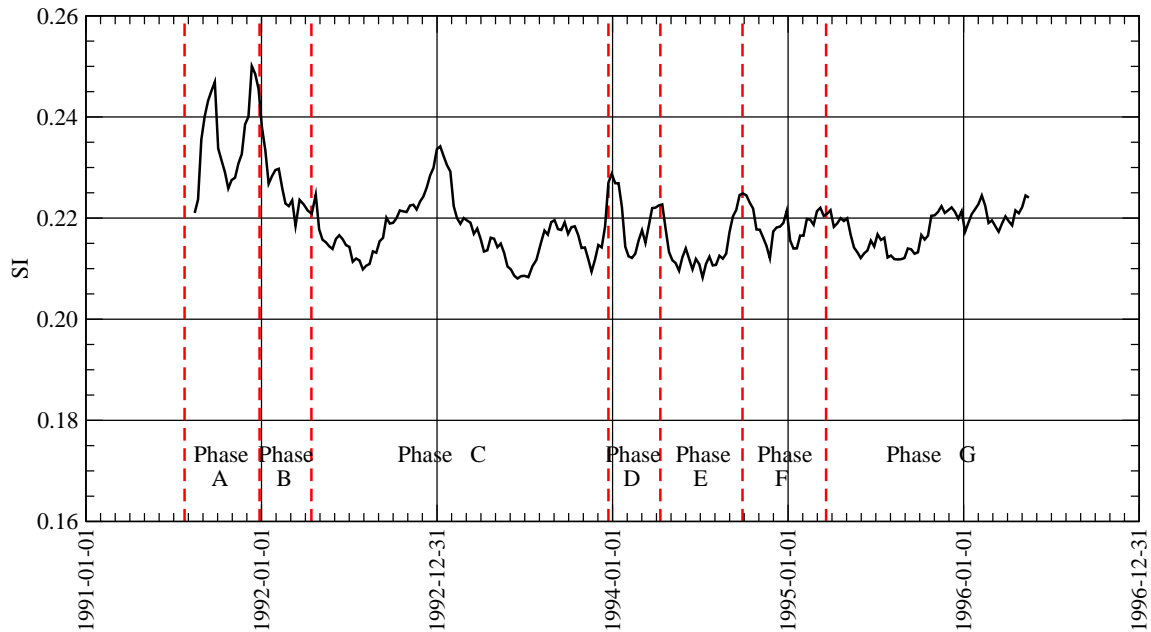


Figure 14: Time history of the 5-week running average of weekly global scatter index of ERS-1 altimeter surface wind speed with respect to the ECMWF ERA-40 re-analysis during the effective lifetime of ERS-1 (August 1991 to May 1996). Various ERS-1 phases are displayed.

3.4 ERS-2 Altimeter OPR Product

Figure 15 shows the time history of the weekly number of super-observations of ERS-2 altimeter OPR products during the period from May 1995 to June 2003. Note that the number of 1-Hz observations averaged to form each super-observation is 11 as was the case for Figure 9. It is clear that apart from several short gaps, the volume of observations was rather constant.

Figure 16 shows the time history of the weekly bias and SI of ERS-2 altimeter SWH with respect to the wave model hindcast (using ERA-40 wind fields before the end of August 2002 and operational wind fields afterwards) during the period from May 1995 to June 2003. In general, ERS-2 OPR SWH seems to be of consistent quality over the whole effective lifetime of spacecraft. The bias shows a seasonal cycle with peaks as high as 16 cm (about 20 cm in 1995 and 1996) in the NH summer and troughs as low as a few centimetres in the winter. The drastic change in bias is due to the use of the higher-quality operational wind fields on 1 September 2002. The SWH SI level is about 16%. There is also a seasonal cycle which is anti-phased with respect to the bias cycle. The amplitude of this cycle is rather small. Again a noticeable change in SI is due to the use of the operational wind fields. It seems that the loss of gyroscopes has no impact on ERS-2 SHW quality.

Figure 17 shows the time history of the weekly relative bias (normalised with model mean wind speed) and SI of ERS-2 altimeter OPR surface wind speed with respect to ERA-40 before the end of August 2002 and the operational wind fields afterwards during the effective lifetime of the satellite (from May 1995 to June 2003). It is clear that until the beginning of 2000, both wind speed bias and SI values were stable. The bias was about +2% of the model mean (about 0.20 m s^{-1}) and the SI was about 21%. Due to an unknown reason, the wind speed bias jumped on 16 January 2000 to more than 10% (about 0.80 m s^{-1}) together with a slight increase in SI. Although a few days earlier, this may not have any connection with the AOCS mono-gyro piloting in early February 2000 (c.f. Féménias and Martini, 2000). However, it is possible that this was an indication of the

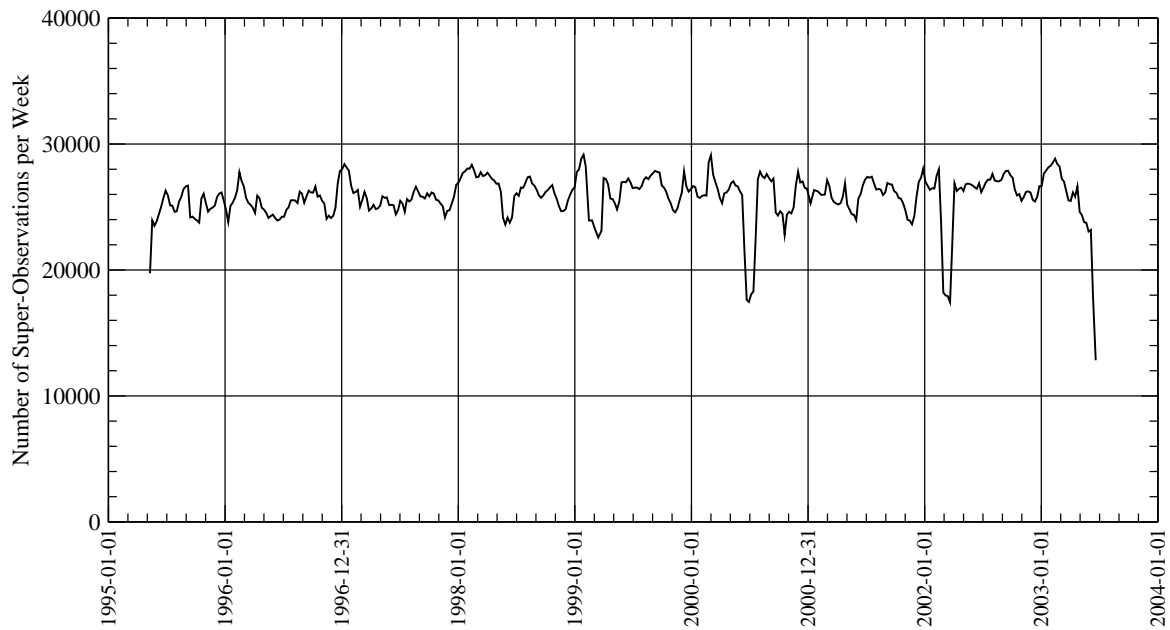


Figure 15: Time history of the 5-week running average of weekly number of ERS-2 altimeter super-observations during the period from May 1995 to June 2003.

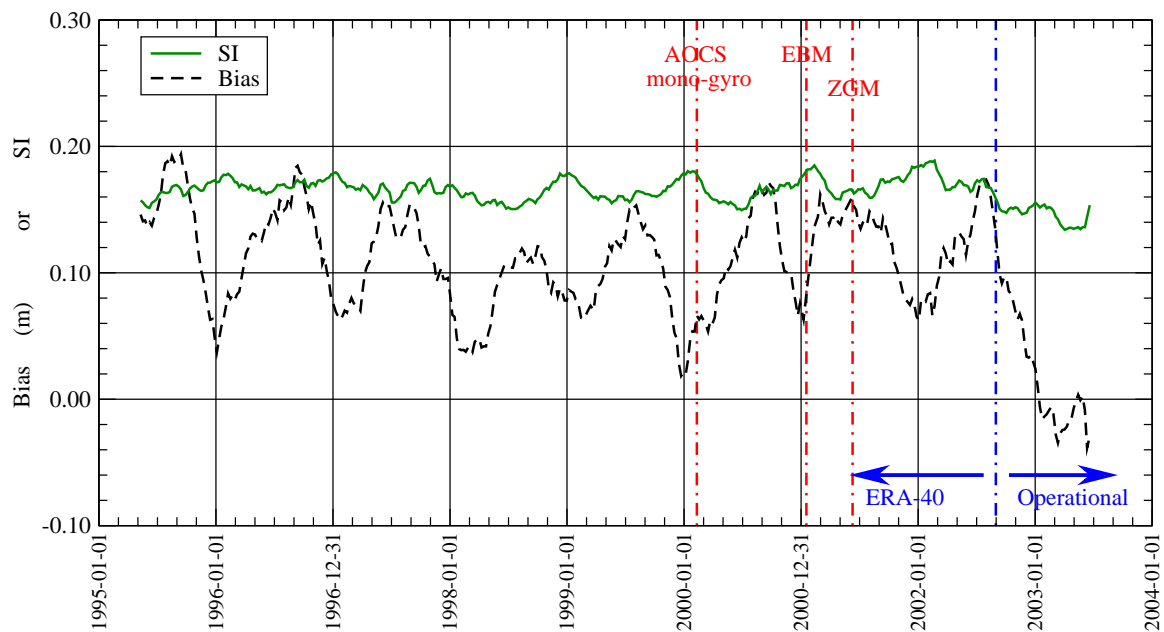


Figure 16: Time history of the 5-week running average of weekly global bias and scatter index of ERS-2 altimeter significant wave height with respect to the ECWAM model hindcast (using ECMWF ERA-40 reanalysis wind fields before the end of August 2002 and operational winds afterwards) during the period from May 1995 to June 2003. Important ERS-2 gyroscope related events are displayed.

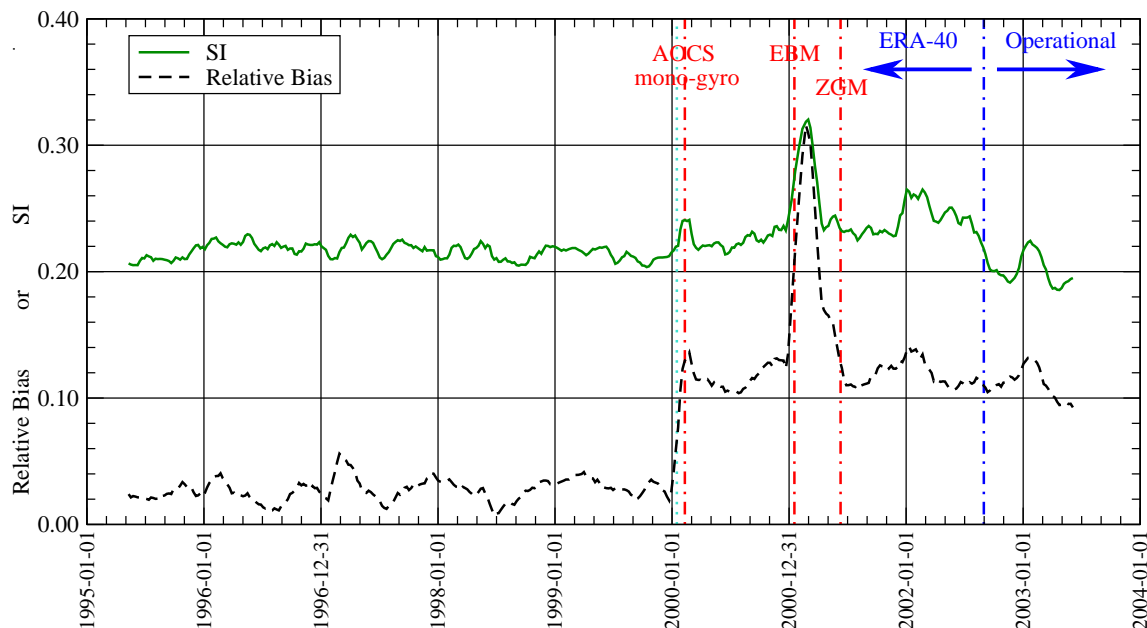


Figure 17: Time history of the 5-week running average of weekly global relative bias and scatter index of ERS-2 altimeter surface wind speed with respect to the ECMWF ERA-40 re-analysis (before the end of August 2002 and operational winds afterwards) during the period from May 1995 to June 2003. Important ERS-2 gyroscope related events are displayed.

forthcoming gyro problems. Further loss of gyroscopes in January 2001, which led to the EBM piloting, further degraded the altimeter wind speeds. An uploaded wrong configuration file after the recovery is responsible for the spike degradation of the product. The impact of using better model wind fields on the bias and SI can be seen after August 2002. The sun blinding effect, which is only effective in the SH, can be noticed in the small spikes around the month of February each year since 2000.

The long-term 5 week running average of weekly global mean backscatter coefficient values over the effective lifetime of ERS-2 shown in Figure 18 is in line with the developments with the wind speed product. The mean backscatter coefficient before January 2000 was stable and fluctuating around a value slightly above 11 dB. After the January 2000 event, the mean value reduced by about 0.2 dB. During the EBM operations the mean backscatter was not stable. The ZGM stabilised this parameter after June 2001.

4 The Synthetic Aperture Radar (SAR) UWA product

For the UWA product, SAR records are provided at 200 km intervals, each containing an image spectrum for an area of about 5 km x 5 km. Records for which all parameters are within an acceptable range are collocated with ECWAM model spectra. The SAR image spectra are then transformed into corresponding ocean-wave spectra using an iterative inversion scheme based on the forward closed integral transformation (MPI scheme, Hasselmann and Hasselmann, 1991). For this procedure the collocated ECWAM model spectra serve as a first-guess. Depending on the outcome of the inversion process, further QC is applied. Long-term monitoring is based on integrated parameters such as the significant wave height, mean wave period and mean directional spread. Monitoring of the one-dimensional energy spectrum is performed as well.

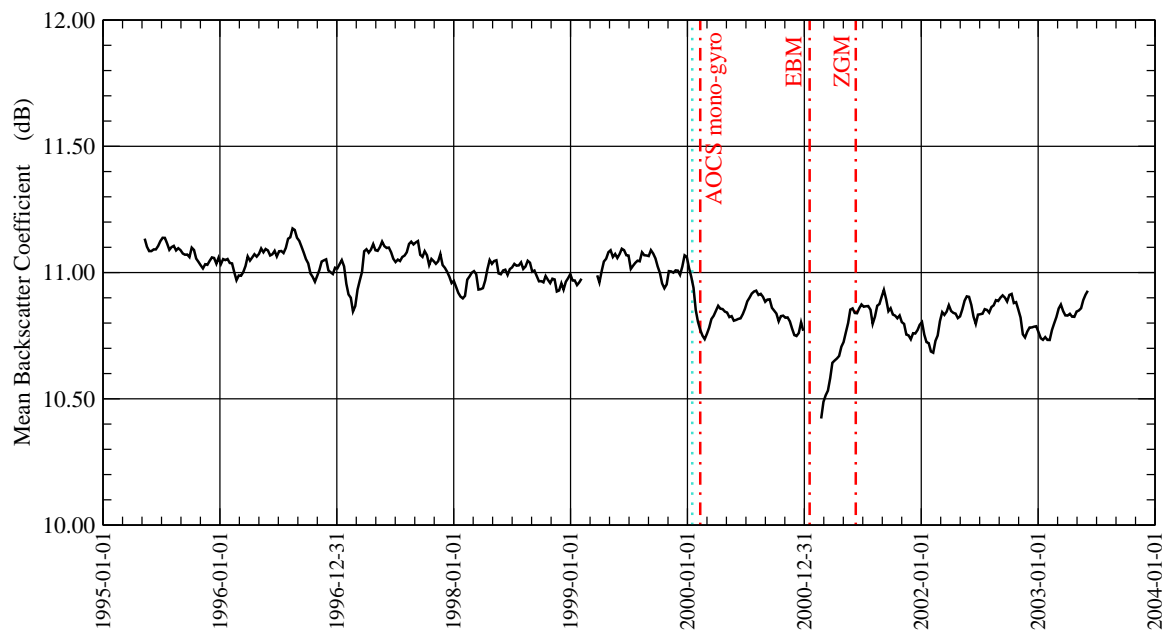


Figure 18: Time history of the 5-week running average of weekly global mean ERS-2 altimeter backscatter coefficient after QC during the period from May 1995 to June 2003. Important ERS-2 gyroscope related events are displayed.

4.1 ERS-2 SAR Data Coverage after June 2003

The loss of the global coverage due to the failure of the on-board low-bit rate tape recorders in June 2003 reduced the number of observations received at ECMWF to about 13% of the full coverage data volume as can be seen in Figure 19 which shows the global weekly number of SAR wave mode spectra processed at ECMWF. The current ERS-2 SAR coverage can be seen in Figure 20. As was done for the altimeter, the extra-tropical Northern Atlantic (north of latitude 20°N) is used for monitoring the FD SAR wave mode UWA product. This is very close to the bulk of the current coverage. The weekly number of SAR wave mode spectra in the North Atlantic since the beginning of the ERS-2 mission is shown in Figure 21. It is clear that the current coverage in the North Atlantic is slightly less than the nominal coverage. The difference is small and is due to the small gap at the southern edge of the North Atlantic. The quality of the products in this area is investigated here.

4.2 ERS-2 SAR Wave Height in the North Atlantic

A long-term monitoring of the significant wave height computed from the inverted ERS-2 SAR spectra was performed. It is worthwhile mentioning that on 28 June 1998 the SAR inversion software was unable to properly handle the SAR data with the new calibration procedure introduced around that time. This was fixed with the implementation of the ECWAM model change on 20 November 2000. Furthermore, SAR data have been assimilated in the wave model since 13 January 2003. Further related events are mentioned in Section 4.4.

Figure 22 shows the time history of the daily bias of the significant wave height computed from the inverted SAR wave mode spectrum with respect to the model wave height in the North Atlantic since April 1996. By ignoring the period with the inversion bug (from 28 June 1998 to 20 November 2000) and the period with EBM (from 17 January 2001 to mid June 2001), it is possible to recognise a seasonal cyclic variation similar to the altimeter SWH (i.e. with minima during the NH winter and maxima during the summer). It is clear that the bias behaviour since the loss of the global coverage is similar to that of 2-3 years before.

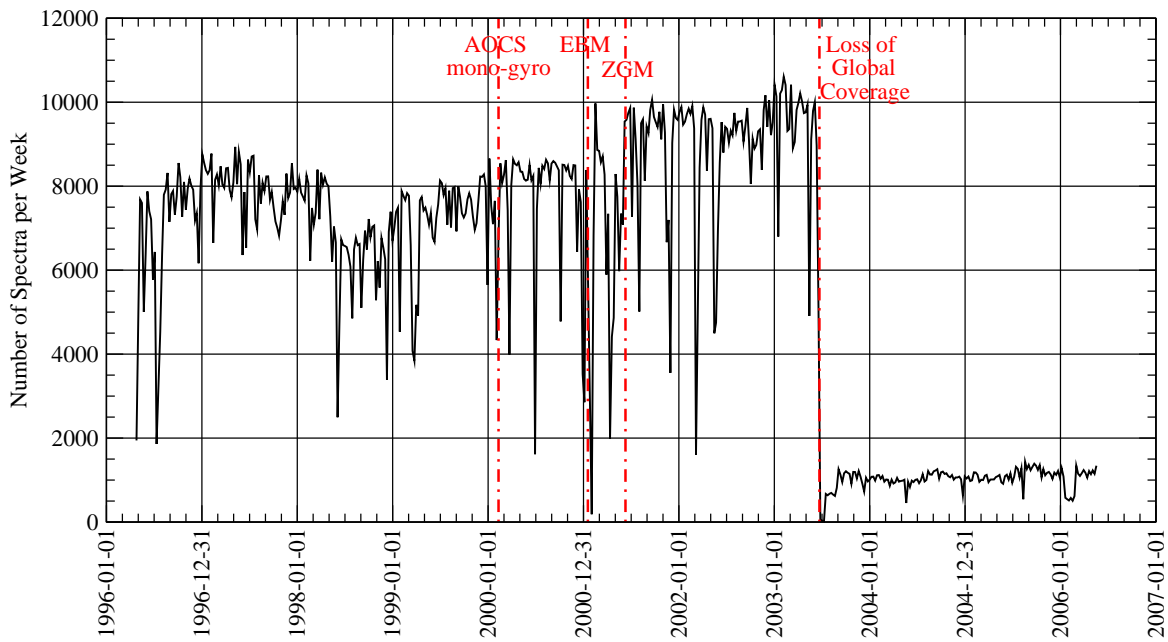


Figure 19: Time history of the global weekly number of ERS-2 UWA spectra during the period from April 1996 to May 2006. Important ERS-2 gyroscope related events are displayed.

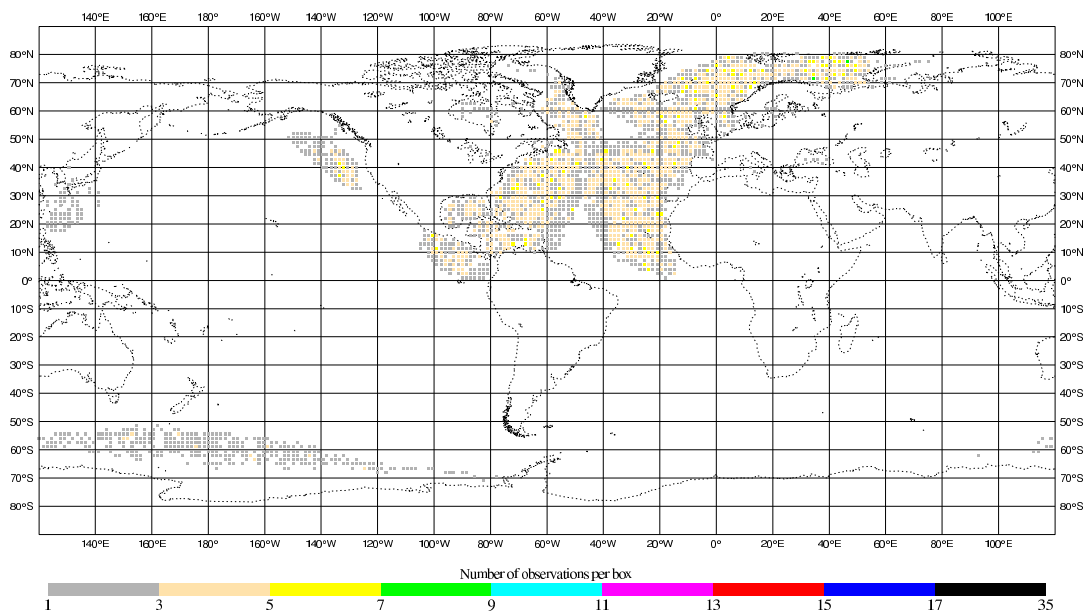


Figure 20: Typical recent ERS-2 SAR wave mode monthly coverage (June 2006).

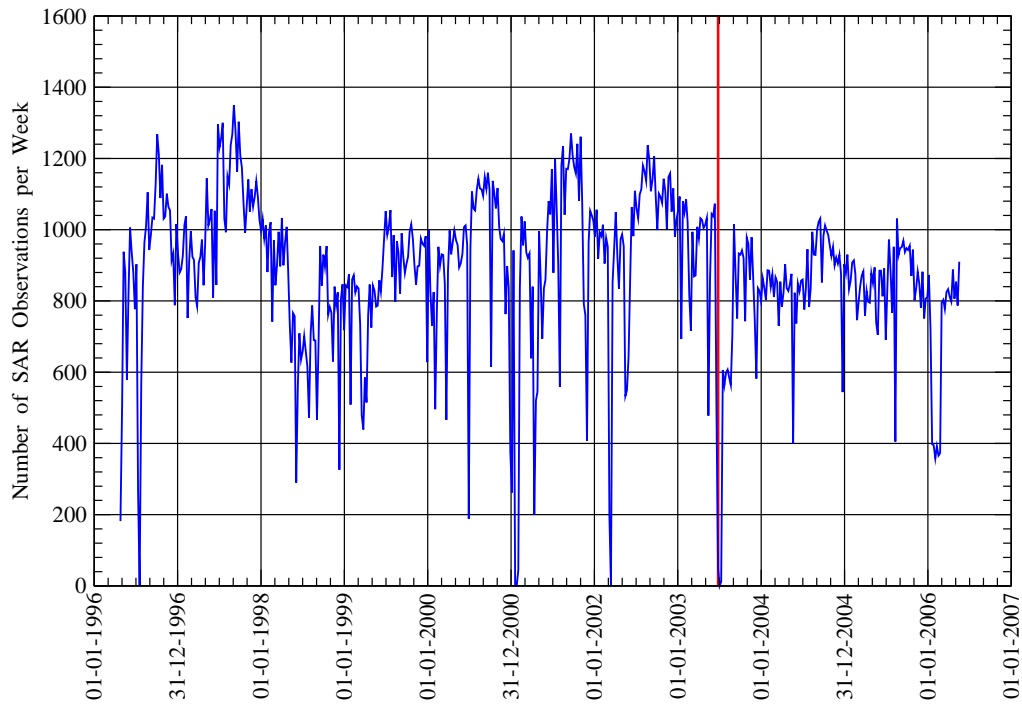


Figure 21: Time history of the 7-day running average of daily number of SAR wave mode spectra in the North Atlantic since 1 January 1996. Date of loss of global coverage is represented by a red thick vertical line.

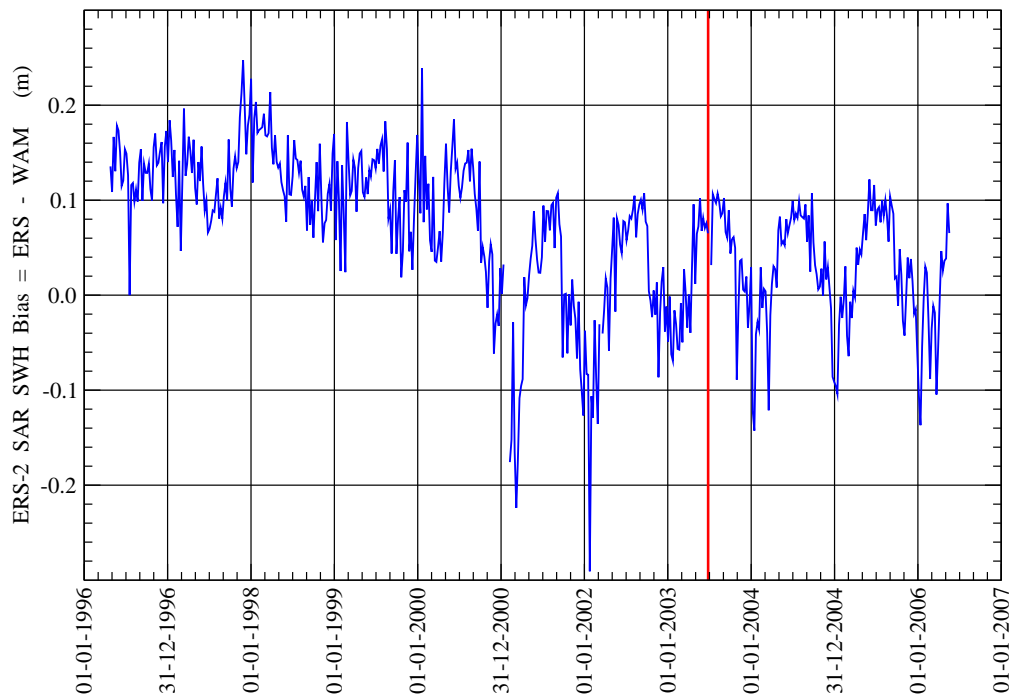


Figure 22: Time history of the 7-day running average of daily bias of SAR wave mode significant wave height with respect to wave model in the North Atlantic since 1 January 1996. Date of loss of global coverage is represented by a red thick vertical line.

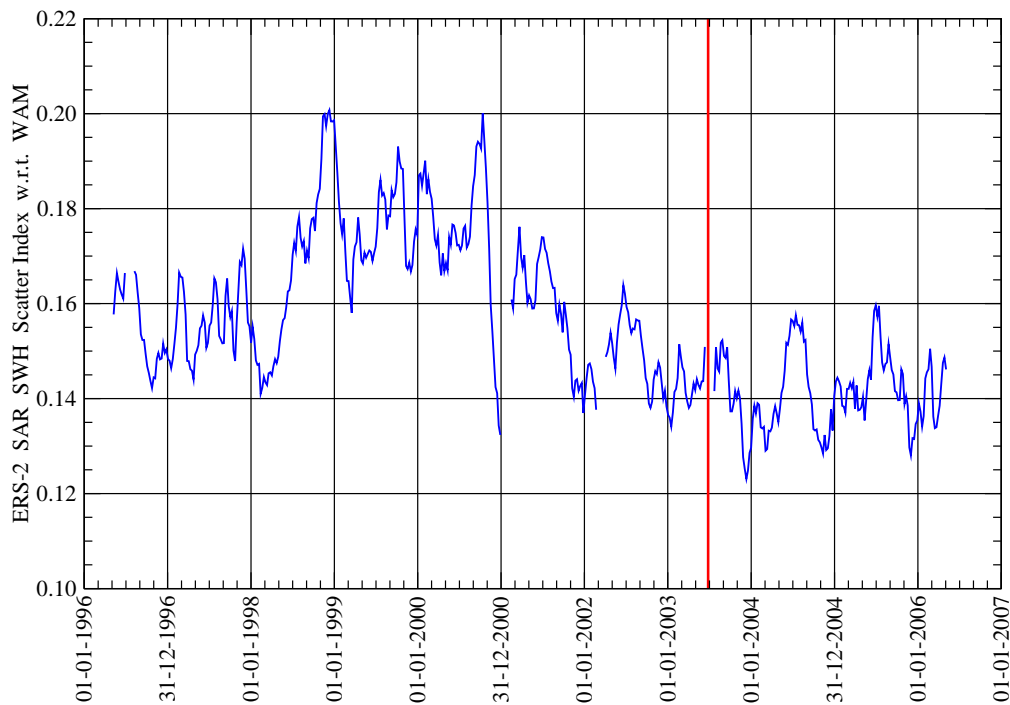


Figure 23: Time history of the 7-day running average of daily scatter index of SAR wave mode significant wave height with respect to wave model in the North Atlantic since 1 January 1996. Date of loss of global coverage is represented by a red thick vertical line.

Figure 23 shows the time history of the daily scatter index of the SWH of the inverted SAR wave mode product with respect to the operational wave model in the North Atlantic since April 1996. There tends to be a kind of seasonal cycle (in phase with the bias cycle) of variation in SI after the recovery from the EBM using the ZGM. This seasonal cycle continued after the loss of the global coverage. Furthermore, the general trend of SI reduction continued over the period of limited coverage. Even the errors became smaller than ever; especially during the winter. This may be a consequence of assimilating the SAR wave mode product in the ECMWF operational wave model since 13 January 2003. A step change in SI can not be seen at that specific date. However, the SI peak values started to be the lowest during the NH summer of 2003.

4.3 Global ERS-1 SAR Significant Wave Height

Figure 24 shows the time history of the weekly number of ERS-1 FD SAR Wave Mode spectra (UWA) products over the entire globe during the period from April 1993 to April 1996. There is no UWA data available at ECMWF before April 1993. The number of observations increased slightly towards the end of 1993.

Figure 25 shows the time history of the weekly bias and scatter index of the SWH derived from the inverted ERS-1 SAR spectra with respect to the operational ECMWF wave model during the period from April 1993 to April 1996. The bias started at a level of about 27 cm before it increased linearly to about 44 cm during July 1993. The reason of this change could not be correlated with any model or SAR related changes. Another linear increase occurred during Phase D (the Second Ice Phase). The bias then fluctuated around 50 cm. The beginning of Phase G (the Second Multi-Disciplinary Phase) witnessed another bias increase to the level of 60 cm. It is clear that almost all phase changes were associated with a local bias change (drop).

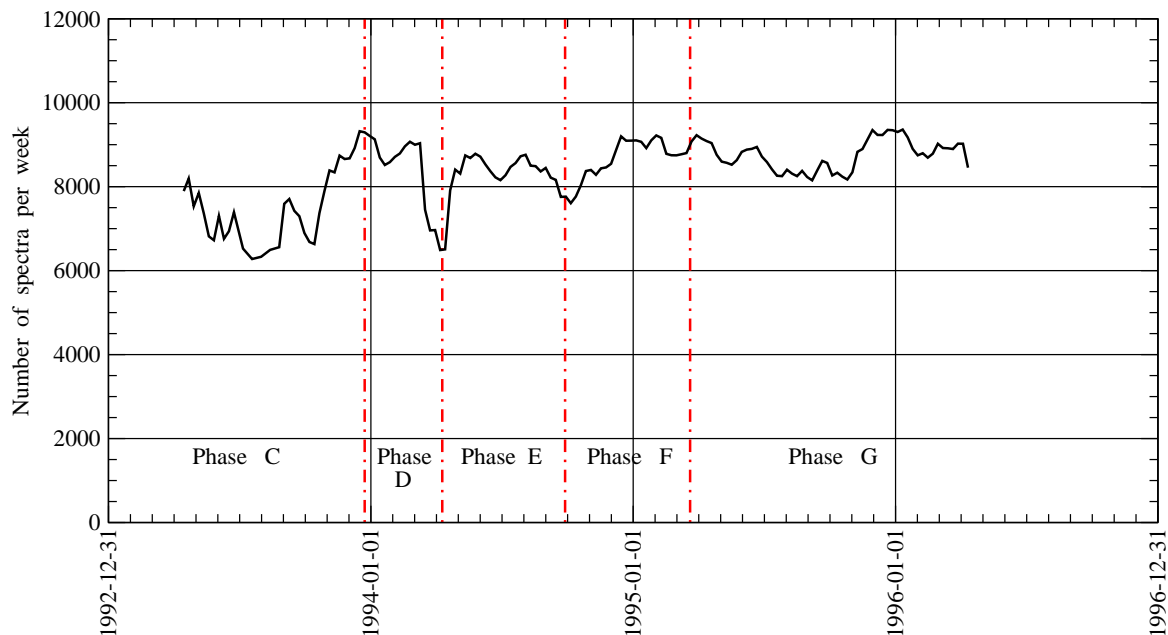


Figure 24: Time history of the 5-week running average of weekly number of ERS-1 UWA spectra during the period from April 1993 to April 1996. Various ERS-1 phases are displayed.

On the other hand, the SI values were small (about 21%) at the beginning. Gradual, but small, increase of SI can be noticed. A significant SI jump happened at the beginning of Phase G together with the last bias jump mentioned above. The SI exceeded 32% during the period from May to September 1995.

It should be noted that one can not rule out the impact of possible undocumented model changes on the observed changes in Figure 25.

4.4 Global ERS-2 SAR Significant Wave Height

The time history of the weekly number of global ERS-2 SAR Wave Mode spectra products during the period from April 1996 to May 2006 is shown in Figure 19. It should be noted that the LBR data coverage of ERS-2 was significantly reduced after the failure of the on-board tape recorders on 21 June 2003. Therefore, as described earlier, any comparison after that date does not represent the global situation.

Figure 26 shows the time history of the global weekly bias and scatter index of the SWH computed from ERS-2 SAR wave mode spectra with respect to the operational ECMWF wave model during the period from April 1996 to May 2006. It is worthwhile reminding that on 28 June 1998 a change in the SAR calibration procedure adversely impacted the SAR inversion process. This was fixed on 20 November 2000. The impact of this bug can be clearly seen in Figure 26. Unfortunately, less than two months after the recovery from this bug, the spacecraft lost its gyroscopes on 17 January 2001 and was piloted, as a result, in the EBM. This resulted in a degraded UWA product during the period of EBM as can be clearly seen in Figure 26. The introduction of the ZGM later that year (June 2003), restored the UWA quality. The loss of the global coverage in June 2003 limited the data to be mainly in the Northern Hemisphere. This fact is reflected into a strong seasonal bias cycle and a mild SI cycle both in phase. Another point to note is the gradual reduction of the SI by time.

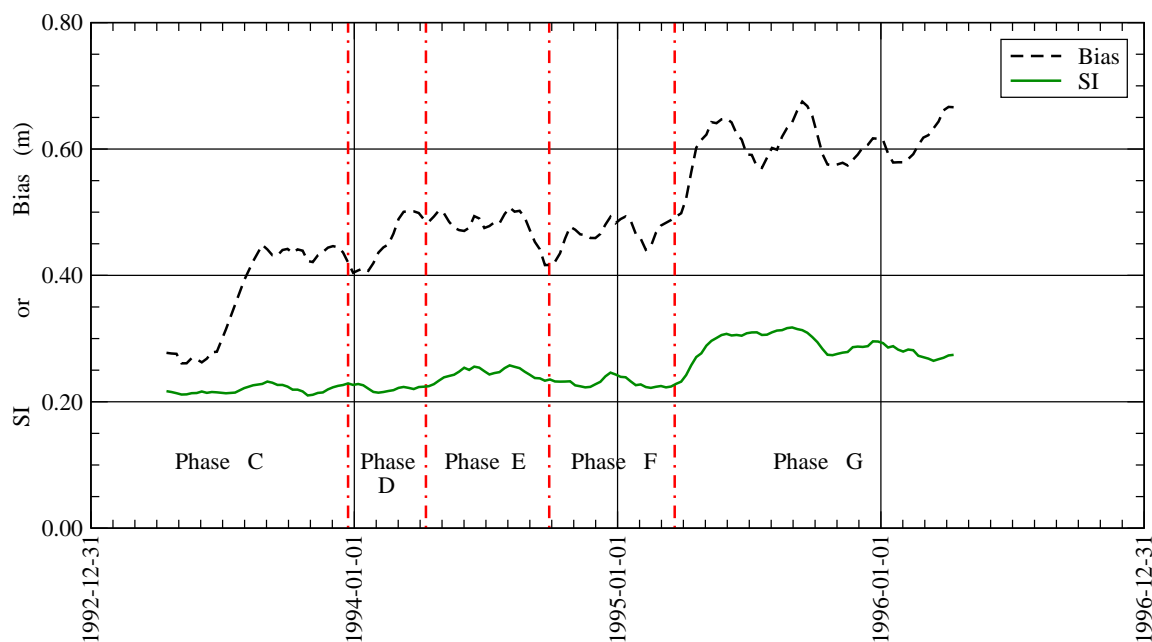


Figure 25: Time history of the 5-week running average of weekly global bias and scatter index of ERS-1 SAR significant wave height with respect to the operational ECMWF wave model during the period from April 1993 to April 1996. Various ERS-1 phases are displayed.

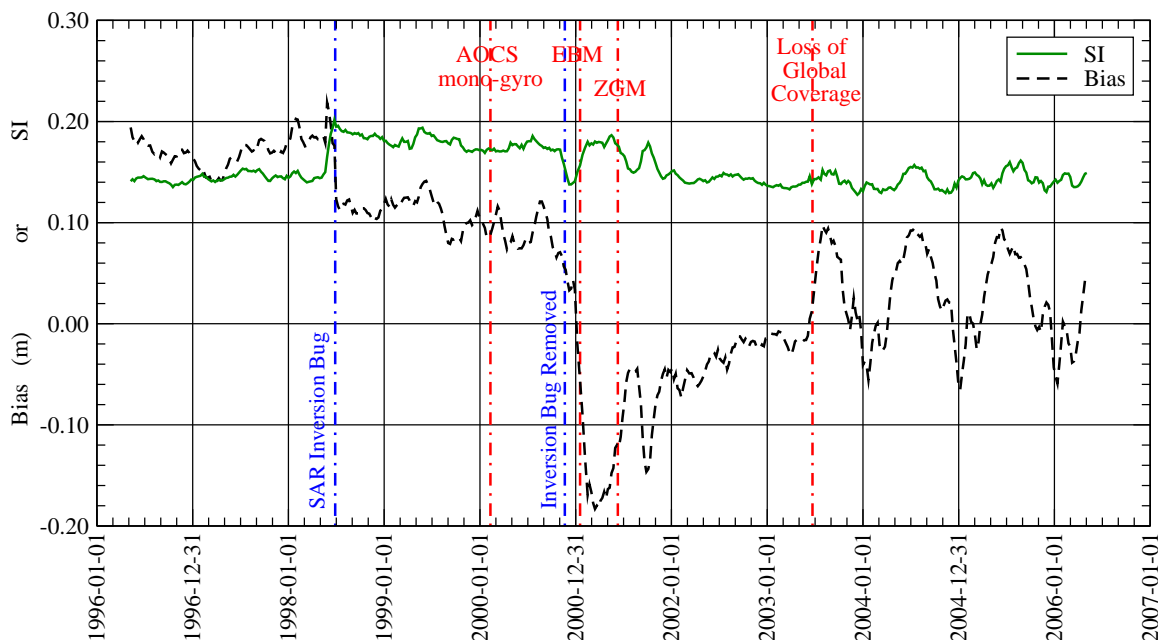


Figure 26: Time history of the 5-week running average of weekly global bias and scatter index of ERS-2 SAR significant wave height with respect to the operational ECMWF wave model during the period from April 1996 to May 2006. Important ERS-2 gyroscope related events and relevant model changes are displayed.

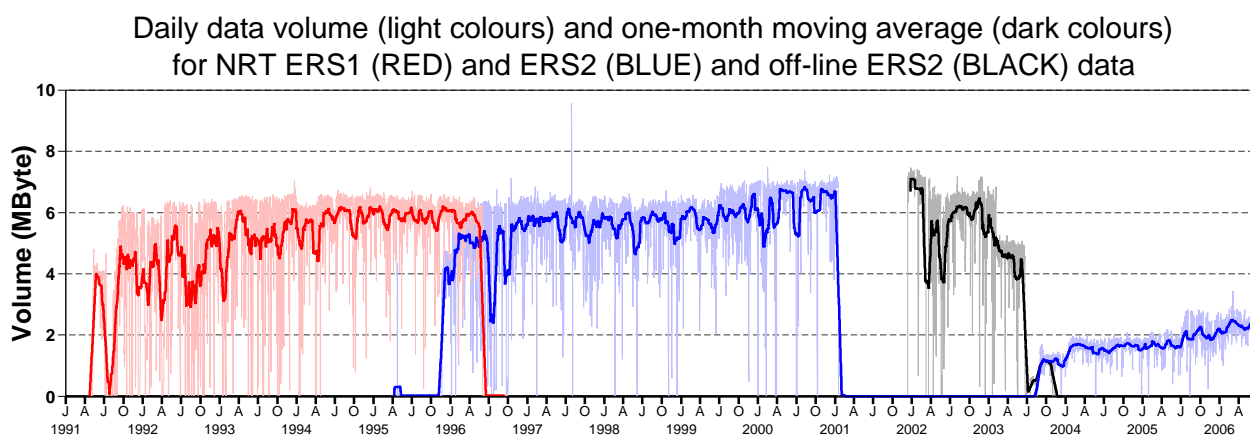


Figure 27: Volume of received ERS-1 and ERS-2 UWI data at ECMWF subject to the data cut-off time in Mbyte per day.

5 The Scatterometer UWI product

5.1 Overview

The AMI instrument on board ERS-2, and previously ERS-1, obtains backscatter measurements from three antennas, illuminating a swath of 500 km, in which 19 nodes define a 25 km product (for details on configuration and geometry see Attema, 1986). From these backscatter triplets, two wind solutions are retrieved one of which is reported in a by ESA disseminated near-real time product, called UWI. For this the geophysical model function CMOD4 (Stoffelen and Anderson, 1997) is used.

ERS-1 was launched on 17 July 1991 and has provided scatterometer data from September 1991 until December 1999. At ECMWF, ERS-1 UWI data was received from 9 May 1991 to 3 June 1996 (red curve in Figure 27), i.e., including some pre-launch test data from 9 May to 4 July 1991. In April 1995 ERS-2 was launched and is still operational. At ECMWF some preliminary data was received on 24 April 1995, while operational data flow started on 22 November 1995 (left-hand blue curve in Figure 27). Due to an on-board anomaly in January 2001, ESA was forced to suspend data dissemination between 18 February 2001 and 21 August 2003. However, off-line data was obtained from ESRIN between 12 December 2001 and 7 November 2003 (black curve in Figure 27). Two months before public re-dissemination, ERS-2 had lost its storage capacity of LBR data, including scatterometer data. After this event, data only remained available when in contact with a ground station. As a consequence, global coverage was lost for the newly disseminated stream, resulting in much lower data volumes (right-hand blue curve in Figure 27).

Within the framework of various contracts with ESA and ESRIN, ECMWF has been monitoring UWI data for a number of years. By passing derived scatterometer winds to the ECMWF operational assimilation system (initially passively, since January 1996 actively), an accurate comparison with model winds can be obtained. Findings of such comparison are, amongst other quality checks, recorded in cyclic reports on 5-weekly intervals. Elements of these reports are described in Section 5.2.

A summary of the monitoring of the entire ERS-2 period will be presented in Section 5.3. It includes a comparison with QuikSCAT data. Seasonal trends in wind speed bias will be discussed in Section 5.4.

Besides being used in the operational data assimilation system, ERS-1 and ERS-2 data have been assimilated in the ECMWF 40-year reanalysis (ERA-40, Uppala *et al.*, 2005). In Section 5.5 results of a triple collocation study of assimilated ERS-1 and ERS-2 winds (1 January 1993 to January 2001), ERA-40 first-guess model winds, and height-corrected buoy data will be presented.

At ECMWF and KNMI the improved geophysical model function CMOD5 had been developed some time ago (Hersbach 2003, Hersbach *et al.* 2004b). In Section 5.6 preliminary results on a refit of CMOD5 will be discussed, that resolves residual biases relative to buoy wind data.

At ESRIN, the entire ERS-1 and ERS-2 record is currently being reprocessed, and for this a new processor (named ASP20) has been developed (Crapolicchio *et al.* 2004). As a check, at ECMWF, some test data from this processor was compared with archived UWI data. Results are presented in Section 5.7.

5.2 5-weekly cyclic UWI ERS-2 monitoring reports

The routine monitoring of the ERS-2 UWI product at ECMWF is summarized in the form of 5-weekly cyclic reports. At <http://earth.esa.int/pcs/ers/scatt/reports/ecmwf/>, these reports are available from Cycle 41 (start date 14 July 1998) up to, at the time of this writing, Cycle 116 (end date 26 June 2006).

Up to Cycle 60 (nominal period) the UWI product has been compared with ECMWF first-guess winds as available within the assimilation system. These FGAT (first-guess at appropriate time) winds are well collocated with the scatterometer observation time and location. From Cycle 69 onwards, e.g., with the start of the reception of offline data from ESRIN, collocation was performed with archived first-guess wind fields instead (available at 3-hourly resolution; and will be called FG winds). Collocation errors are slightly larger, but on the other hand it enables the monitoring of data that does not pass pre-assimilation quality control.

From Cycle 69 onwards, the quality of winds inverted on the basis of CMOD5 are monitored as well. At ECMWF, such retrieved ERS-2 scatterometer winds have been assimilated from 9 March 2004 onwards.

The ECMWF scatterometer cyclic monitoring reports contain the following elements:

- An introduction, giving a general summary of the quality of the UWI data and trends w.r.t. previous cycles. Data coverage, and interruptions in data reception are listed. Also, since Cycle 69 (12 November 2001) it is mentioned whether there was an enhancement of solar activity, and whether it could have affected the UWI wind product. Finally, it is informed whether the ECMWF assimilation system has changed and whether this had an anticipated impact on the quality of the ECMWF surface winds.
- A section giving a detailed description of performance during the cycle. It includes the following plots.
- Evolution of 5-weekly averaged performance of the cone distance, bias and standard deviation of UWI and CMOD4 wind speed and direction compared to ECMWF FG winds starting from Cycle 69. The plot for Cycle 116 is given in Figure 28.
- Data coverage and geographical averages of UWI wind speed, and relative bias and standard deviation compared to ECMWF FG winds (Cycle 91 onwards; for Cycle 116, see Figure 29).
- Backscatter (σ_0) bias for the three beams (fore, mid, aft) as function of across-node number (1 to 19) and stratified with respect to ascending and descending tracks:

$$dz = \langle z \rangle / \langle z_{\text{CMOD}}(\theta, \text{FGAT}) \rangle,$$

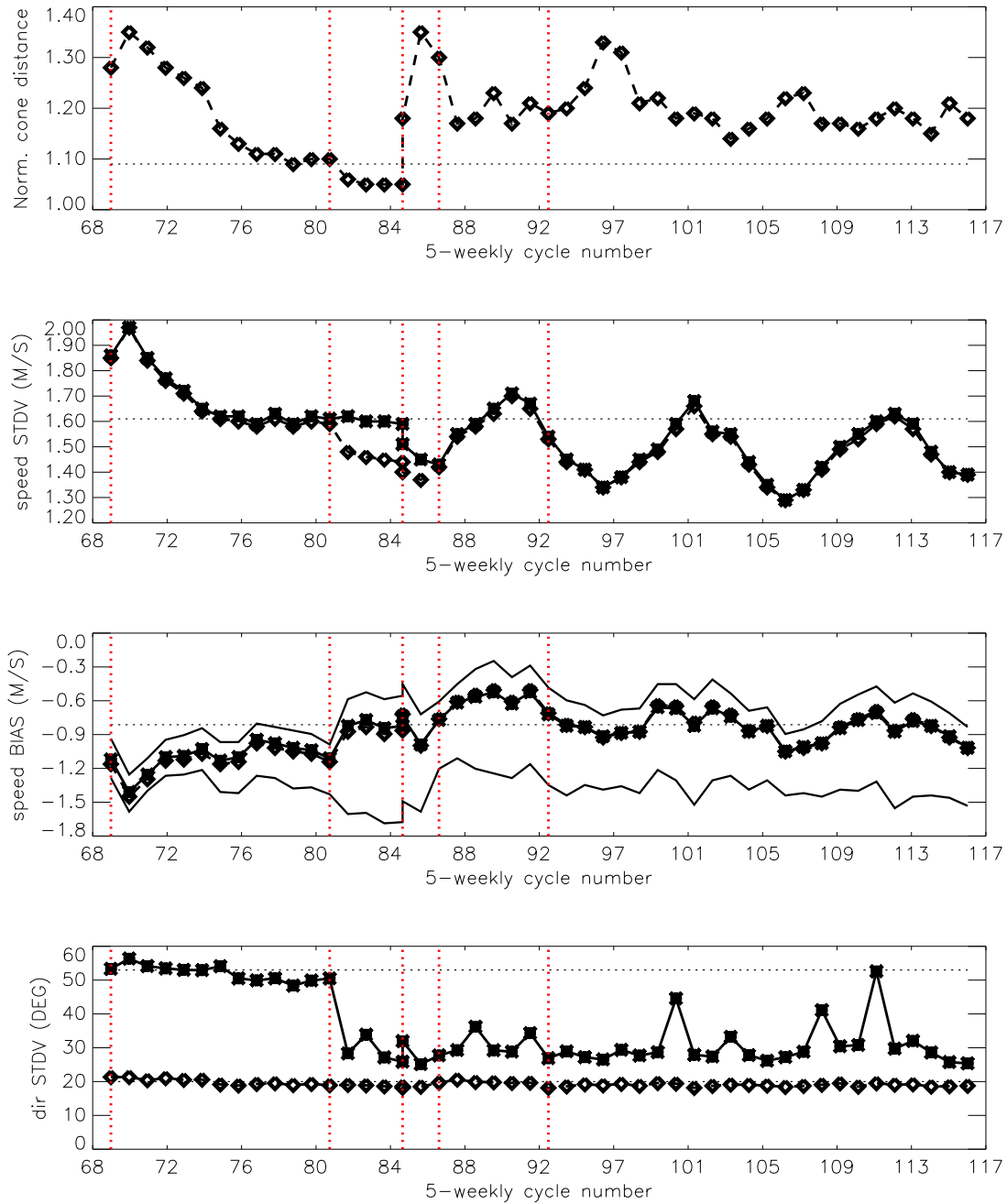


Figure 28: Evolution of the performance of the ERS-2 scatterometer averaged over 5-weekly cycles from 12 December 2001 (Cycle 69) to 26 June 2006 (end Cycle 116) for the UWI product (solid, star) and de-aliased winds based on CMOD4 (dashed, diamond). Results are based on data that passed the UWI QC flags. For Cycle 85 two values are plotted; the first value for the global set, the second one for the regional set (see text for more details). Dotted lines represent values for Cycle 59 (5 December 2000 to 17 January 2001), i.e. the last stable cycle of the nominal period. From top to bottom panel are shown the normalized distance to the cone (CMOD4 only) the standard deviation of the wind speed compared to FG winds, the corresponding bias (for UWI winds the extreme inter-node averages are shown as well), and the standard deviation of wind direction compared to FG.

where $z = \sigma_0^{0.625}$, and θ the node and beam-dependent incidence angle. This bias depends on the underlying model function. Results are produced on the basis of CMOD4. Trends in the inter-node and inter-beam relationship indicate changes in the antenna patterns, because trends in the normalizing ECMWF winds would appear as integral shifts. Examples (Cycle 110 and 116) are given in Figure 30.

- Time series of the difference between the fore and aft incidence angle of node 10 (Cycle 81 onwards), and the UWI k_p -yaw quality flag (Cycle 88 onwards). Asymmetries indicate errors in yaw attitude control.
- Plots of time series of quantities averaged over 6-hourly data batches and stratified w.r.t. six classes of nodes (1-2, 3-4, 5-7, 8-10, 11-14 and 15-19) of
 - The normalized distance to the cone, the fraction of rejected data on the basis of CMOD4 inversion, ESA flags or ECMWF land and sea-ice mask, and the total number of received data over sea.
 - Bias and standard deviation of UWI versus ECMWF first-guess winds for wind speed and direction.
 - The same for CMOD4 winds as inverted at ECMWF from level 1b.
- Global plots of locations where UWI winds were more than 8 m s^{-1} weaker or stronger than ECMWF FG winds (included from Cycle 79). Usually two specific cases are highlighted in a separate plot.
- Accumulated histograms (scatter plots) between UWI and ECMWF first-guess wind speed and direction. Scatter plots for FG winds versus de-aliased CMOD4 winds and CMOD5-based winds have been produced from Cycle 74 onwards. Examples for a one-year accumulation period (1 July 2005 to 30 June 2006) are presented in Figure 31.
- Time series for at ECMWF assimilated CMOD5 winds, and QuikSCAT winds relative to ECMWF FGAT winds for a region covering the North Atlantic and part of Europe (Cycle 94 onwards; for Cycle 116 see Figure 33).

5.3 General Overview for ERS-2

22 November 1995 - 19 March 1996

Pre calibration phase. Large but constant σ_0 biases were encountered.

19 March 1996 - 6 August 1996

End of commissioning phase. A thorough calibration has resulted in revised look-up tables. Scatterometer data from ERS-2 (bias-corrected CMOD4 winds) is included in the ECMWF assimilation system on 1 June 1996, replacing the assimilation from ERS-1 that had been used from 30 January 1996. Details may be found in Isaksen and Janssen (2004).

6 August 1996 - 18 June 1997

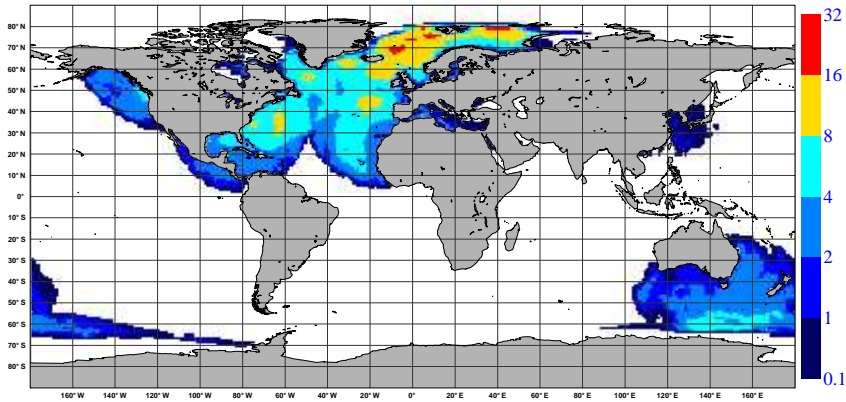
Due to an erroneous switch to a redundant calibration subsystem σ_0 values increase by 0.2 dB, leading to wind biases $\sim 0.5 \text{ m s}^{-1}$.

18 June 1997 - 17 January 2001 (Cycle 22 to Cycle 60)

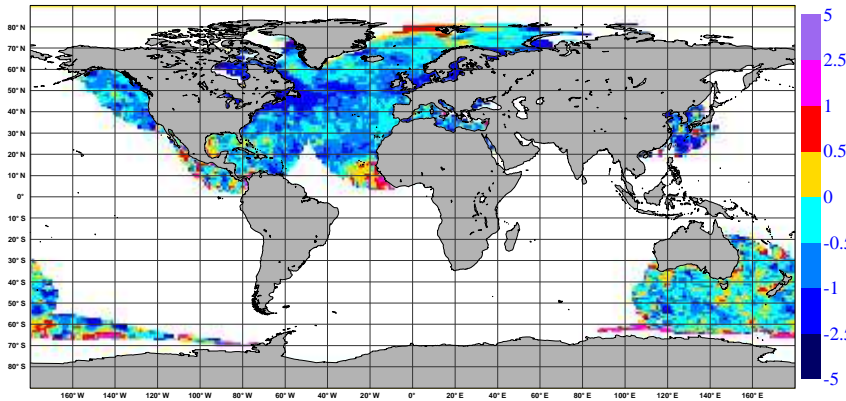
Nominal period. Backscatter values return to old, well-calibrated levels.

The performance of the UWI product is stable, although in the fall of 2000 there are some problems with the functioning of several of the six gyroscopes on-board the spacecraft. On average, backscatter levels are around 0.5 dB too low, leading to winds that are on average $0.7\text{-}0.8 \text{ m s}^{-1}$ slower than FGAT winds. Although the inter-node and inter-beam sigma biases are small, the UWI wind-speed bias does depend on node number (from

NOBS (ERS-2 CMOD5), per 12H, per 125km box
average from 2006052300 to 2006062618 GLOB:3.15



BIAS (ERS-2 CMOD5 vs FIRST-GUESS), in m/s.
average from 2006052300 to 2006062618 GLOB:-0.43



STDV (ERS-2 CMOD5 vs FIRST-GUESS), in m/s.
average from 2006052300 to 2006062618 GLOB:1.22

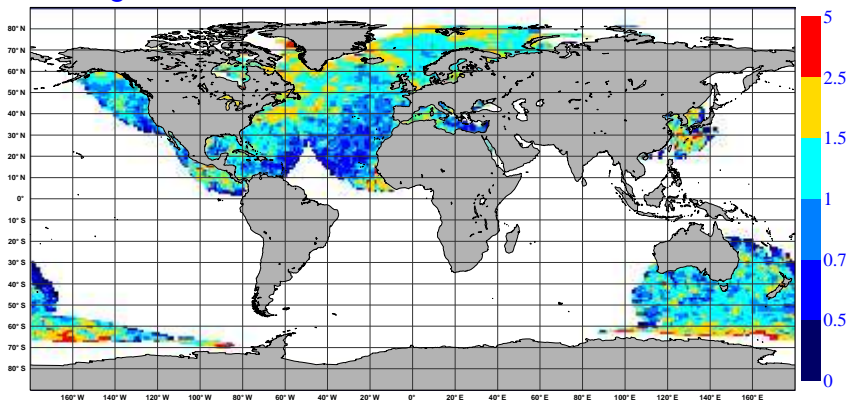


Figure 29: Average number (top) of observations per 12H and per N80 reduced Gaussian grid box (~ 125 km), relative bias (middle) respectively standard deviation (lower panel) compared to ECMWF FG 10-meter winds, (~ 125 km) of UWI winds that passed quality control at ECMWF for data in Cycle 116 (23 May - 26 June 2006). Only data are plotted for grid cells that contained at least 5 observations.

-1.1 ms^{-1} for low to -0.6 ms^{-1} for high incidence angle). It is induced by imperfections in the CMOD4 model function (and do not appear for CMOD5). Standard deviation between UWI and FGAT winds are around 1.6 ms^{-1} . For Cycle 59, values of the average cone distance, (UWI - FGAT) and (CMOD4 - FGAT) statistics are displayed by the horizontal dotted lines in Figure 28.

17 January 2001 - July 2001 (Cycle 60 to 65)

As a result of the on-board failure there are no gyroscopes left for the platform's attitude control. The control system is switched to Extra Back-up Mode. The dissemination of scatterometer data is suspended after 2 February 2001; empty cyclic reports are made for Cycles 62 to 68.

July 2001 - 12 December 2001 (Cycle 65 to 69)

Introduction of the Zero-Gyro Mode (ZGM). Satellite pointing is achieved through payload data and the digital earth sensor. Although pitch and roll can be controlled accurately, large errors in the yaw attitude (several degrees) still occur. Such errors especially affect the quality of the scatterometer measurements. Dissemination of scatterometer data remains suspended.

12 December 2001 - 4 February 2003 (Cycle 69 to 81).

Restart of dissemination of UWI data, however, to a restricted group of users only. At ECMWF, the monitoring is resumed. Existing tools are updated where necessary.

Large errors in yaw, which especially seem to occur around periods of enhanced solar activity, have a large negative impact on the data quality. During these events, part of the backscatter signal is destroyed, which, after inversion, results in far too low winds. Peaks of more than -3 ms^{-1} frequently occur, especially in January 2002 (Cycle 70), which marks a period of considerable solar activity. These incorrect data are also visible in the scatter diagrams of UWI versus FG wind speed as anomalously large numbers of collocations between strong ECMWF winds and weak UWI winds. For later cycles the situation improves.

Initially, also extremely large negative biases are observed in the backscatter levels, including data that was less affected by yaw errors. Large inter-node and inter-beam differences induce large cone distances. The situation is worst for Cycle 70 but later slowly improves. However, the increasing negative bias towards higher nodes remains. In line with the average reduction in σ_0 bias, the cone distance and wind-speed biases gradually improve (see Figure 28).

For the random error of the UWI and CMOD4 wind speeds a similar trend is observed: worst for Cycle 70 (almost 2 ms^{-1}) and then first improving rapidly and later stabilizing. From Cycle 75 onwards its level is around the value obtained for the nominal period (see Figure 28). In general best results are obtained for winds inverted on the basis of CMOD5. Both the negative bias level and standard deviation are smaller for such derived winds.

The performance in wind direction is found to be much less affected. Although initially wind direction performs somewhat worse, at Cycle 72 it is on the level of the nominal period, and after Cycle 75 it has even become better (see lower panel of Figure 28).

4 February 2003 - 22 June 2003 (Cycle 81 to 85)

Start of the validation phase of ESACA, the new processor. Aim of this complete revision of the original LRDPF, was to bring the quality of the UWI product back to its nominal level. It is capable of the interpretation of on-board filter characteristics appropriately according to an estimation of the yaw attitude error. During the test phase, ESACA data is distributed for Kiruna station only, which leads to daily data gaps between approximately 21 UTC and 06 UTC.

The new de-aliasing algorithm, being part of ESACA, (and developed at DNMI) appears to perform well. The UWI winds agree considerably more often to the wind solution that is closest to the ECMWF FG wind

direction. Values of standard deviations drop from 50 to less than 30 degrees (see Figure 28).

The UWI winds do not coincide anymore with one of the two solutions from the CMOD4 inversion at ECMWF. At ECMWF inverted CMOD4 winds appear to be of much higher quality than the by ESRIN disseminated UWI winds (see Figure 28). At ESRIN, the cause for this non-ideal situation is tracked down quickly. At the beginning of April 2003 appropriate corrections to ESACA are implemented and since then UWI winds are in line with CMOD4 again (though not yet for Kiruna station; i.e., the discrepancy in winds remains for the data as received at ECMWF). The standard deviation w.r.t. FGAT winds are below 1.50 ms^{-1} , i.e., about 0.1 ms^{-1} better than it used to be during the nominal period.

Large fractions of high k_p values are found, especially for nodes at high incidence angles (more than 50%). Consideration between the (UK) MetOffice and ESRIN reveals that there is a problem with the BUFR encoding algorithm. A solution is formulated and implemented (again, not yet at Kiruna).

In the near range the fore and aft beam show large negative biases in the average backscatter levels. As a result, very large negative wind-speed biases are found for low nodes (-1.6 ms^{-1}). At ESRIN its cause is identified and resolved (though, not visible at Kiruna). Apart from the initially large near-range biases, the inter-node and inter-beam differences in backscatter levels are small. Their level is comparable to that during the nominal period.

The incidence angles between the fore and aft beam are not equal anymore. They now show a rapid variation in time and peaks up to 7 degrees are observed. This asymmetry is a direct result of errors in yaw attitude. A large anomaly on April 1 2003 (while the Earth was inside a gusty solar wind stream, source: www.spaceweather.com) results in low-quality winds. This event illustrates the potential usefulness of a yaw flag in the UWI product.

Along with improved quality of the CMOD4 winds, the normalized distance to the cone is now below the level of the nominal period.

22 June 2003 - 21 August 2003 (Cycle 85 to 87)

On 22 June 2003 the second Low Bit-Rate recorder on-board ERS-2 fails, and is found to be beyond repair. As the first recorder had become unusable in December 2002, this means that now there is no facility left to store LBR data, including scatterometer data. After a data-void period of three weeks, data flow is resumed on 16 July 2003, however, only for observations for which there is a direct contact with a ground station. For the Kiruna test data received at ECMWF, this means that coverage is limited to the Atlantic north of 40°N , making statistics very sparse.

21 August 2003 - 26 June 2006 (Cycle 88 to 116)

On 21 August 2003, the public dissemination of UWI data is restarted. This fortunate event makes an end to the restricted distribution. From this date onwards data is received in the original manner (via the UK Met-Office), and is stored in the usual ECMWF analysis-input archives (the restricted data had been archived at a less accessible location). The original monitoring in the assimilation system (e.g., comparison with FGAT winds) is restored. However, cyclic reports are still based on the off-line monitoring (FG winds), since it includes data that is rejected in an early stage of the assimilation system. Besides Kiruna station, data is now also received from Maspalomas, Gatineau and Prince Albert, which, bearing in mind the loss of the LBR recorders, results in a coverage over the North Atlantic, part of the Mediterranean, the Gulf of Mexico, and a small part of the Pacific north-west from the US and Canada. An initial gap in the North Atlantic is resolved on 15 January 2004, when a station at West Freugh (Scotland) is included. Coverage in the Caribbean is obtained by a station at Miami (February 2005), in the Chinese Sea by a station at Beijing (July 2005), and partial coverage over the Southern Hemisphere by the inclusion of McMurdo (Antarctica, June 2005) and Hobart (Tasmania, February 2006) stations. All joined together lead to a (for Cycle 116) coverage as indicated in Figure 29. The areas

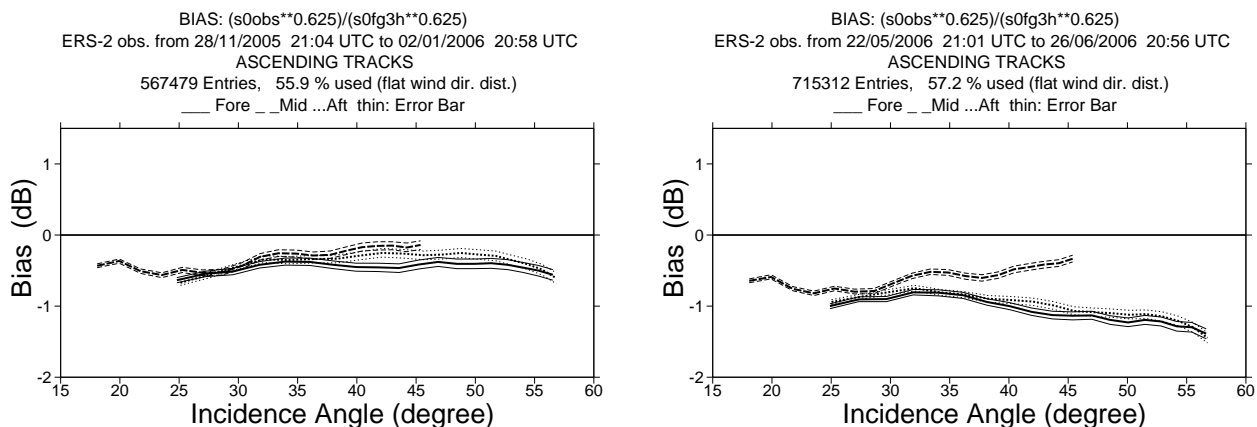


Figure 30: Ratio of $\langle \sigma_0^{0.625} \rangle / \langle \text{CMOD4}(\text{FGAT})^{0.625} \rangle$ converted in dB for the fore beam (solid line), mid beam (dashed line) and aft beam (dotted line), as a function of incidence angle for and ascending tracks of data within Cycles 111 (left panel) and 116 (right panel). The thin lines indicate the error bars on the estimated mean.

covered by Miami and Beijing station allow for the accurate observation of a number of tropical cyclones.

The recording by separate ground stations means that in certain areas observations are reported more than once. For each ground station gridding into 25-km cells and de-aliasing is performed separately. It is found that overlapping cells may be dislocated (by 12.5 km), and that regularly not the same wind solution is selected for all ground stations.

The operational ESACA processor has resolved all non-optimal features that had been detected during the validation period. Data quality is found to be high, although the cone distance has increased and is now 10% higher than for nominal data (see top panel of Figure 28). Assimilation experiments with winds inverted on the basis of CMOD5, show a small positive impact in global forecast skill (Hersbach *et al.* 2004a). It leads to the re-introduction of ERS-2 scatterometer data in the ECMWF assimilation system on 8 March 2004.

An original flag for high k_p values is now also set for yaw attitude errors exceeding 2 degrees. It appears to work well and a close correlation with the asymmetry in incidence angle is observed.

Since the loss of global coverage, a seasonal trend has been introduced in the now regional data set, making objective monitoring more difficult. A clear example of such a trend is observed for the relative standard deviation of the UWI wind speed compared to FG winds (see second panel of Figure 28); a more intense and volatile wind climate in winter time will naturally lead to an increased RMSE.

A seasonal trend also appears for bias levels of both wind speed and backscatter. For backscatter, bias patterns are found to be flat in winter time (at levels that are less negative than for nominal data), but large asymmetries emerge during summer. Typical examples for this consistent yearly trend are given in Figure 30. For wind speed, bias relative to ECMWF FG winds, are found to be (like backscatter) most negative around July ($\sim 1.1 \text{ m s}^{-1}$) and least negative around January ($\sim 0.7 \text{ m s}^{-1}$). In the next Section, this issue will be studied in some detail.

Yearly averaged (over all 19 nodes) UWI winds are about $0.8 - 0.9 \text{ m s}^{-1}$ biased low compared to ECMWF FG winds (see e.g., top left-hand panel of Figure 31 for the period July 2005 - June 2006). This is slightly more negative than for nominal data (before January 2001), and is probably due to a gradual slight increase in average wind speed of the ECMWF first-guess winds. This trend emerges, e.g., from longterm monitoring of QuikSCAT winds and of buoy winds (not shown). For CMOD5, average wind bias is around -0.35 m s^{-1} .

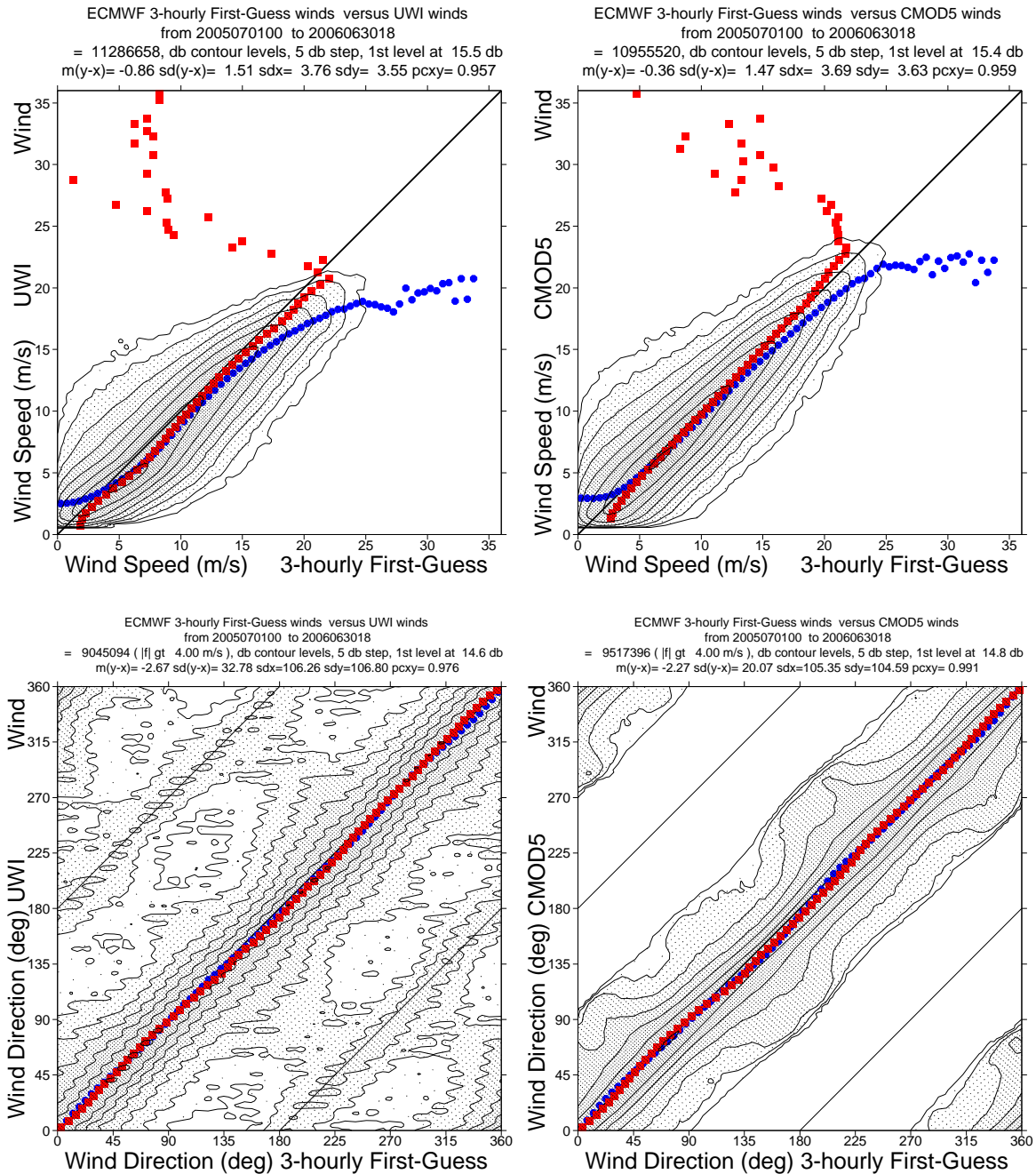


Figure 31: Two-dimensional histogram of UWI (left hand panels) or de-aliased CMOD5 (right hand panels) relative to ECMWF FG for wind speed (top panels) and wind direction (lower panels) over the one-year period from 1 July 2005 to 30 June 2006. Blue circles denote averages for bins in the x-direction, and red squares averages for bins in the y-direction.

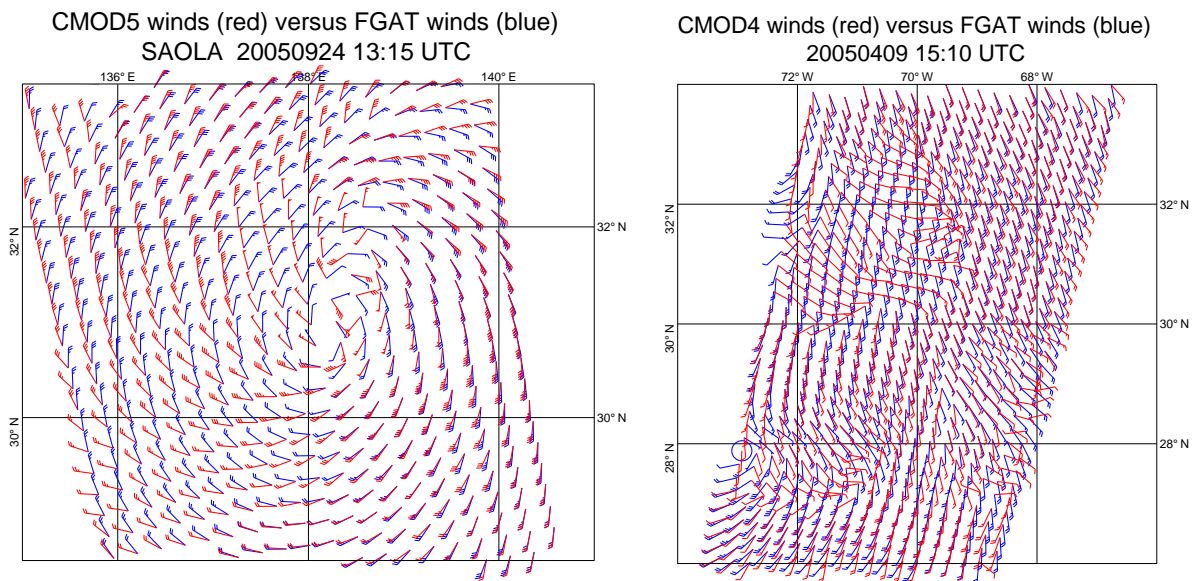


Figure 32: Two examples for situations where scatterometer and ECMWF winds differ significantly.

This relative bias seems fairly independent on wind speed, as e.g. can be seen from the histogram displayed in the top right-hand panel of Figure 31. The one-year accumulated relative standard deviation of UWI winds is about 0.1 m s^{-1} lower than for nominal data (1.5 m s^{-1} versus 1.6 m s^{-1}), but this can be the result of the omission of the strong winds in the Southern Hemispheric storm tracks, combined with the gradually improved quality of ECMWF winds.

As observed during the ESACA test phase, the quality of UWI wind direction is (as a result of the improved de-aliasing algorithm) superior to that of nominal data (see lower panel of Figure 28). Nevertheless, incorrect wind solutions are still frequently reported as can be seen from the lower panels of Figure 31. Occasionally, peaks of degraded performance occur, which usually can be traced back to temporarily missing input (model winds) in the ESACA de-aliasing software. Such peaks are not observed for at ECMWF de-aliased CMOD5 winds.

A previously non-existing bias is observed for wind direction. On average, (de-aliased) ERS-2 winds are found to be rotated by 3 degrees counter-clockwise compared to ECMWF first-guess fields. One reason for this consistent bias appears the lack of cross-isobar flow (Hollingsworth 1994) at warm advection of ECMWF surface winds. A similar, opposite, effect is found on the Southern Hemisphere, and, therefore, this bias is averaged out in a global verification. A study for QuikSCAT data versus model winds may be found in Brown *et al.* 2005.

Locations for large differences between UWI (or CMOD5) winds are usually isolated. They often indicate meteorologically active regions, for which UWI data and ECMWF model field show reasonably small differences in phase and/or intensity. Tropical cyclones and frontal systems are typical candidates. One example is the observation of typhoon Saola from Beijing ground station on 24 September 2005, which is displayed in the left panel of Figure 32. Hardly affected by rain, the ERS-2 scatterometer winds are able to provide a detailed picture. It shows that ECMWF first-winds are, besides suffering from a lack of cross-isobar flow, too weak near the cyclone centre.

Besides large differences that pin point errors in the ECMWF first-guess field, occasionally cases are observed in which UWI winds seem clearly incorrect. This is often manifested as odd patches within a surrounding wind

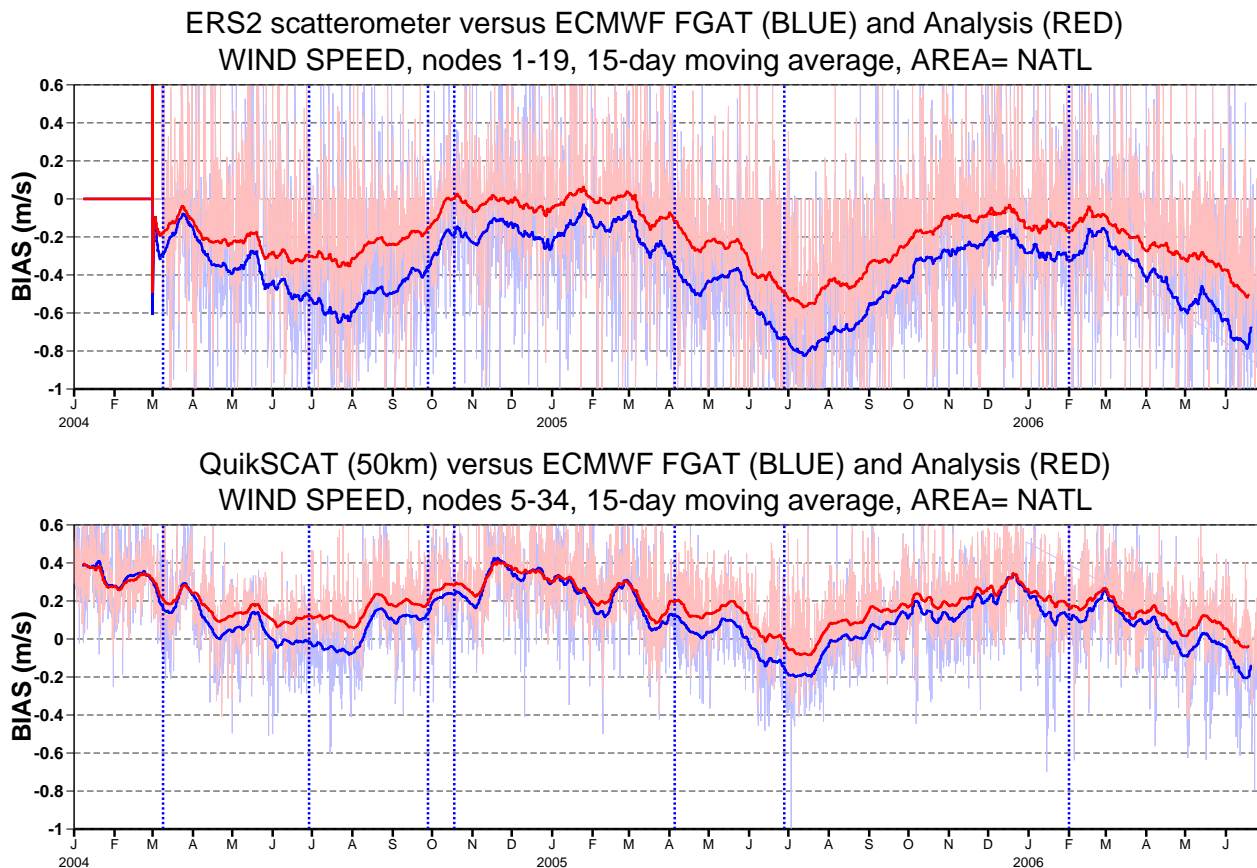


Figure 33: Wind-speed bias relative to FG winds for actively assimilated ERS-2 winds (based on CMOD5) for nodes 1-19 (top panel) respectively 50-km QuikSCAT (based on the QSCAT-1 model function and reduced by 4%) for nodes 5-34 (lower panel), averaged over the area (20N-90N, 80W-20E), and displayed for the period 01 January 2004 - 26 June 2006. Fat curves represent centred 15-day running means, thin curves values for 6-hourly periods. Vertical dashed blue lines mark ECMWF model changes.

field that looks sensible. An example is shown in the right-hand panel of Figure 32. Problems are found most likely to occur at light wind conditions relatively close to land, and at lower incidence angles in general.

5.4 Seasonal fluctuations in wind speed bias

The evolution in wind bias of the regional data set can also be well-observed from the monitoring of the wind product as used in the ECMWF assimilation system. Figure 33 presents a time series for ERS-2 (based on CMOD5), and QuikSCAT data (50-km product based on QSCAT-1 model function, minus 4% bias correction) restricted to an area that is well-covered by ERS-2. It shows that a similar (though somewhat weaker) trend for the regional ERS-2 data is also found for QuikSCAT data. This indicates that the variations have probably a geophysical nature, and therefore do not indicate changes in the ERS-2 antenna pattern. Several reasons for the yearly trend can be suggested. One obvious contribution is the fact that a scatterometer measures wind via the surface stress. Direct transformation from surface stress to 10-metre wind (called equivalent neutral winds) does not take local stability effects into account. Typically, in unstable conditions, equivalent neutral winds are about 0.2 m s^{-1} stronger, and vice versa for stable conditions. Since (ECMWF) model 10-metre winds do

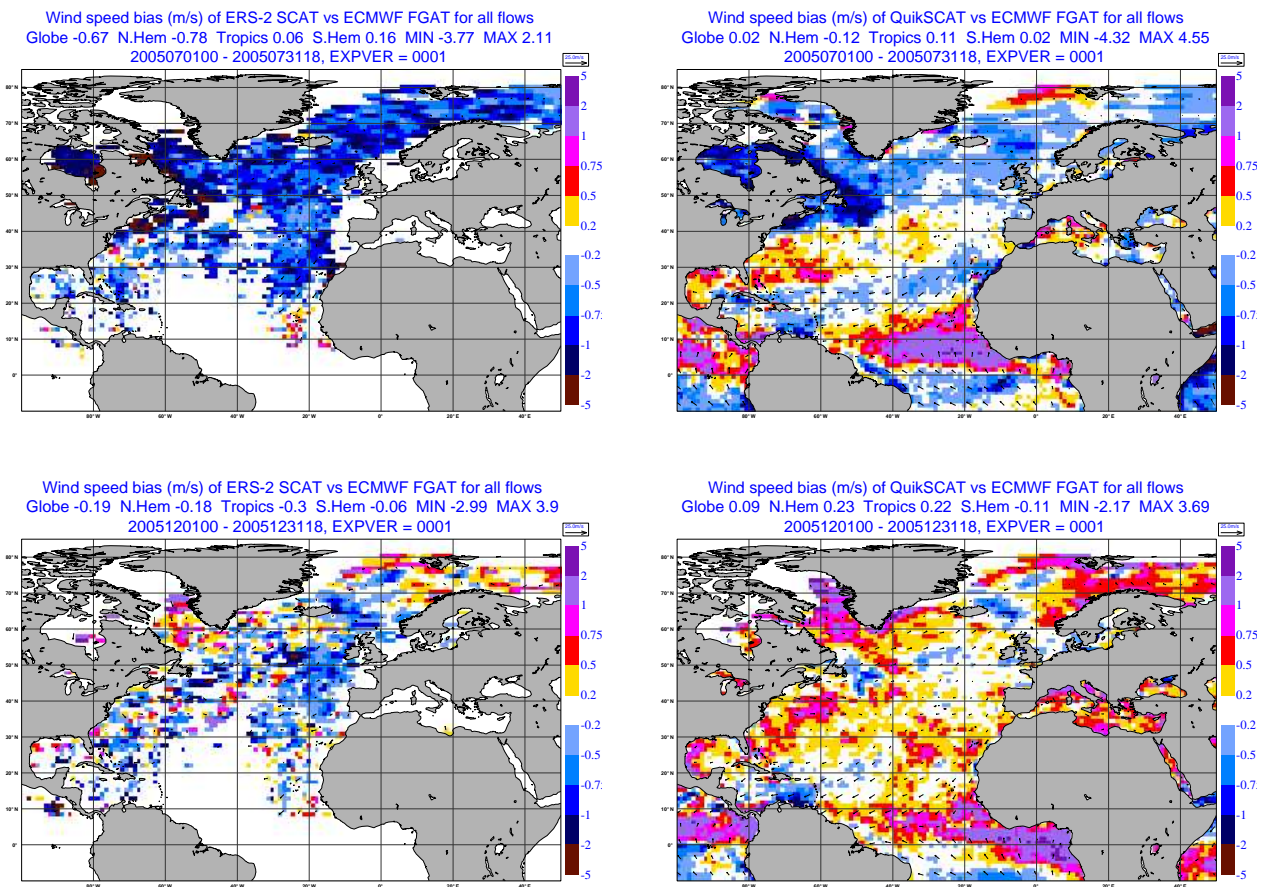


Figure 34: Bias relative to ECMWF first-guess fields for actively assimilated ERS-2 (left-hand panels) and QuikSCAT (right-hand panels) scatterometer data, averaged over July 2005 (top panels) and December 2005 (lower panels).

include stability effects this introduces case-dependent differences.

In Figure 34, maps of monthly averaged relative bias are presented for ERS-2 (left-hand panels) and QuikSCAT (right-hand panels) for July 2005 (top panels) and December 2005 (lower panels), e.g., at the extremes of the inter-annual variations. For July 2005 it displays a large negative bias around New Foundland for both ERS-2 and QuikSCAT data. These concern on average warm southerly winds, flowing over a cooler ocean surface, and therefore creating an on average, stable stratification. As a consequence, equivalent neutral (scatterometer) winds are weaker than the (ECMWF) surface winds which induces an apparent negative bias. In winter, the opposite is observed. Now off-land winds are colder than the sea surface, leading to unstable stratification. As a result, equivalent winds are stronger than the actual surface winds, resulting in a relative positive bias. The geographical distribution as displayed in Figure 34 is typical. The negative bias around New-Foundland in July, e.g., is observed every year.

The difference between neutral and non-neutral winds only explains part of the yearly bias trend. When ECMWF winds are converted to neutral winds a comparison with scatterometer winds still shows residual stability effects. An example is illustrated in Figure 35, where NRT QuikSCAT winds as provided by JPL (i.e. on original 25-km grid and JPL retrieved vector wind) are compared to ECMWF 10-m neutral winds (obtained

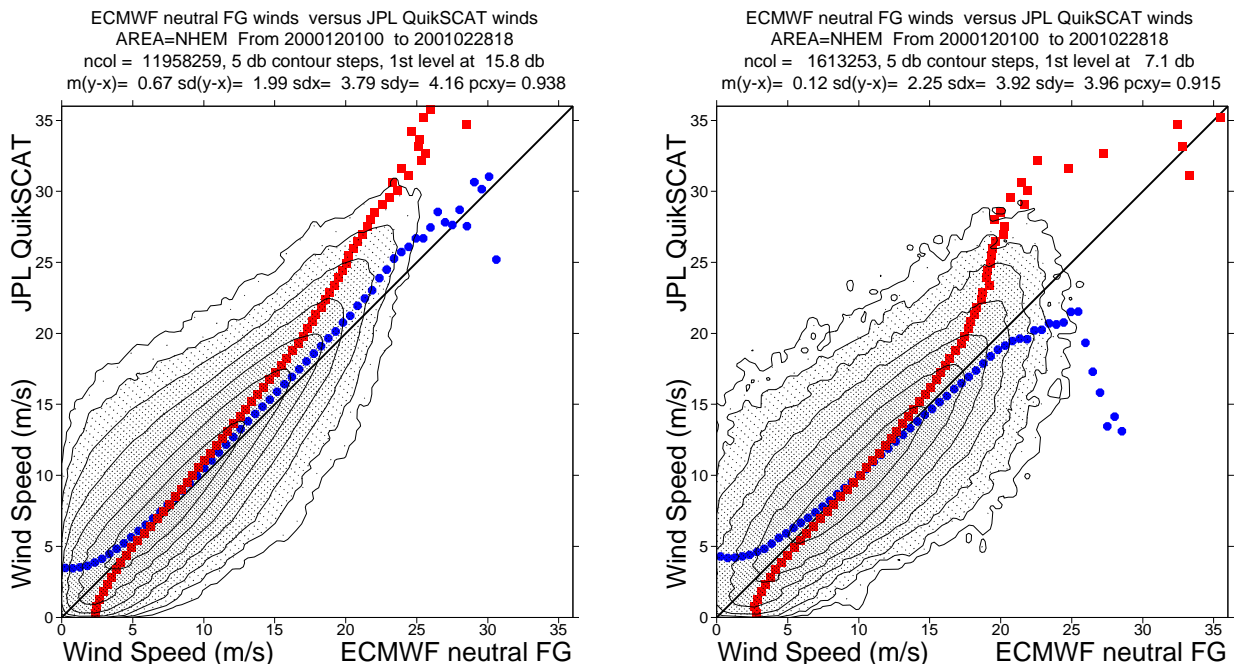


Figure 35: Scatter plot of NRT NESDIS QuikSCAT product versus equivalent neutral ECMWF first-guess winds over the Northern Hemisphere for December 2000 to February 2001 for unstable winds (left panel) and stable winds (right-hand panel). Blue circles denote averages for bins in the x -direction, and red squares averages for bins in the y -direction.

U.S. National Data Buoy Center (NDBC)									
41001	41002	41010	42001	42002	42003	44004	44008	44011	46002
46004	46005	46006	46035	51001	51002	51003	51004	46059	
Canadian Marine Environmental Data Service (CMEDS)									
46036	46184								
Met Office (UKMO)									
62029	62081	62105	62106	62108	64045				

Table 1: Five-digit WMO identifiers of buoys that were taken in consideration for the collocation with UWI winds, grouped into originating data provider.

from information at lowest model level and the sea surface; see IFS Documentation, 2004, Chapter IV.3.2 for details). Data is stratified into an unstable (left-hand panel) and a stable class (right-hand panel) according to the sign of the model surface buoyancy flux. In addition, only data on the Northern Hemisphere for one season (December 2003 to February 2004) is considered to ensure a similar geographic coverage within both classes (for a global and longer set each stratification class will appear in specific areas/seasons which could introduce spurious correlations). It shows that the relative bias is 0.67 ms^{-1} for unstable and 0.12 ms^{-1} for unstable winds, i.e., a difference of 0.55 ms^{-1} . In case ECMWF winds are not converted to equivalent neutral winds, this difference appears to be 1.03 ms^{-1} (not shown). Therefore, the obvious correction for neutral effects explains about half of the variation in bias. The remainder could be due to stability-dependent errors in the ECMWF boundary layer formulation (see Brown *et al.* 2006). However, differences could also arise from non-resolved dependencies in the relation between scatterometer backscatter and surface stress. Dependencies could, e.g., be found on the seastate, such as the steepness of ocean-surface waves. More insight on this issue could be obtained from a comparison with a third, independent data set. Buoy winds are the obvious candidate.

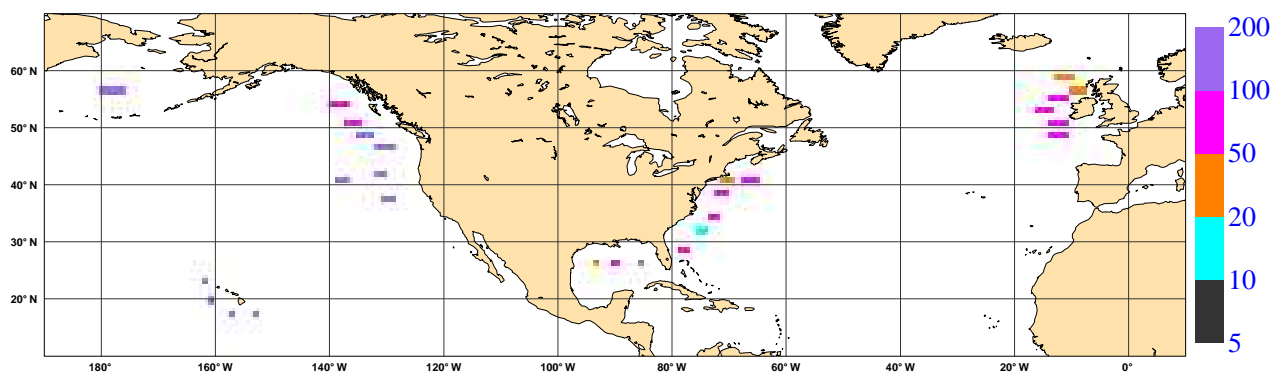


Figure 36: Number of collocations over August 1995 for which buoy and ERS-1 UWI location are within 30 minutes and 50 km.

5.5 Overview of the ERS-1 and ERS-2 scatterometer product by collocation with Buoy data and ERA-40 winds

Scatterometer data from both ERS-1 and ERS-2 have been assimilated within the ECMWF ERA-40 re-analysis (Uppala *et al.*, 2005) from 1 January 1993. Instead of using the provided UWI wind solution, AMI winds were determined in-house by first bias correcting level 1B backscatter values, then inverting on the basis of CMOD4, and finally bias correcting the obtained wind solutions. This product will be denoted by ECMOD. During the ERS-2 period (22 November 1995 to 17 January 2001), the level of bias correction for backscatter was adapted several times, in order to counterbalance for known calibration problems in the level-1B UWI product. An example is the pre-calibration phase (up to 19 March 1996). For ERS-1 bias files were held constant for the entire period (1 January 1993 to 3 June 1996).

Although the changing observational network has improved the quality of the reanalysis model fields over time considerably, the numerical model and assimilation method were fixed during the entire period. This facilitates the path for an objective long-term inter-comparison between ERS-1 and ERS-2 data. For this, the (in FEEDBACK files) available UWI and ERA-40 FGAT wind pairs are collocated with wind observations from buoy platforms. All buoys as received via GTS at ECMWF are considered for which long-term monitoring routinely performed at ECMWF has revealed confidence on their quality (Bidlot *et al.*, 2002). Only buoys with observation height between 4 and 10m, being far enough from land and for which data was reported during most of both the ERS-1 and ERS-2 periods are included. As a result, 27 platforms remain, covering an area around Hawaii, the U.S. and Canadian East and West coasts, and Northern Europe. Buoy WMO identifiers are presented in Table 1, and their locations in Figure 36. Wind speed at buoy observation height is transformed (Bidlot *et al.*, 2002) to 10-m height by applying a logarithmic profile, using a Charnock constant of 0.018 (other values in that range give very similar results).

Using an at ECMWF developed collocation package, all locations are found for which (ERA-40 FGAT, UWI) pairs are separated by less than 50 km and 30 minutes from the 27 selected buoys. On average, about 2,000 collocations are found per month (see lower panel of Figure 38). Only for the overlap period between ERS-1 and ERS-2 (22 November 1995 to 3 June 1996), much lower amounts are obtained. This is due to a too low upper limit on the number of allowed ERS scatterometer winds in the ERA-40 assimilation system.

From the collocation set, statistics between the various sources of wind information (UWI, ECMOD, buoy, and ERA-40 FGAT) can be evaluated and compared. Figure 37 shows results for wind speed. The top panel shows the bias of UWI (black), ECMOD (red) and ERA40 FGAT (blue), relative to the buoy observations.

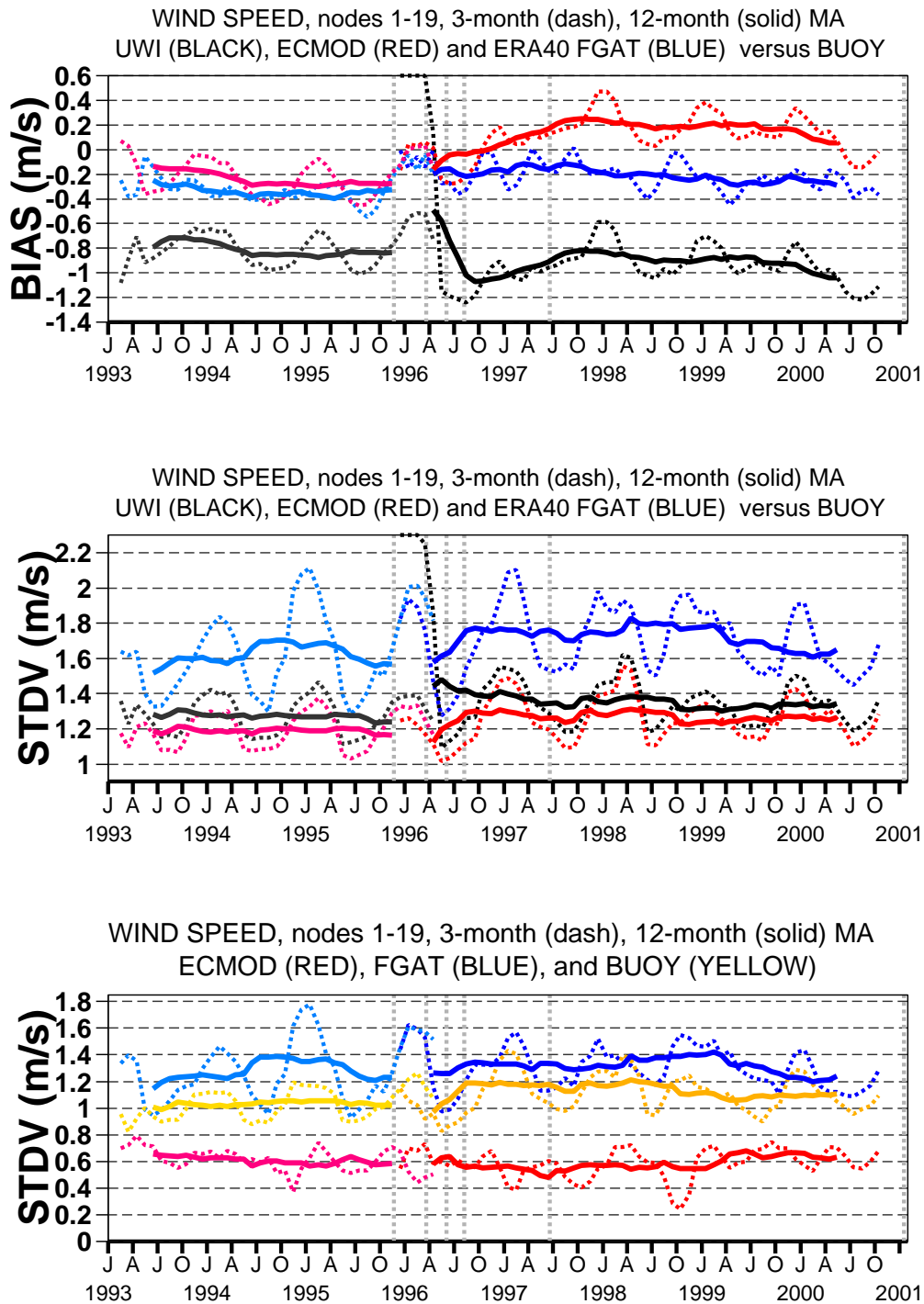


Figure 37: Time series for ERS-1 and ERS-2 UWI (black) at ECMWF assimilated product (ECMOD, red) and ERA-40 FGAT (blue) winds versus buoy wind speed (relative bias in top and standard deviation in middle panel). Based on triple collocation, the lower panel displays estimates of random errors for the individual wind sources (buoy in yellow). Dash curves represent 3-monthly mean averages; solid curves 1-yearly mean averages. Lighter colours are for ERS-1, darker colours for ERS-2. Grey vertical lines mark (in chronological order) the start of assimilation of ERS-2 (22 November 1995), the end of the ERS-2 pre-calibration phase (19 March 1996), the last date of assimilation of ERS-1 (3 June 1996), the switch to a redundant calibration sub-system (6 August 1996), and the nominal ERS-2 period (18 June 1997 to 17 January 2001).

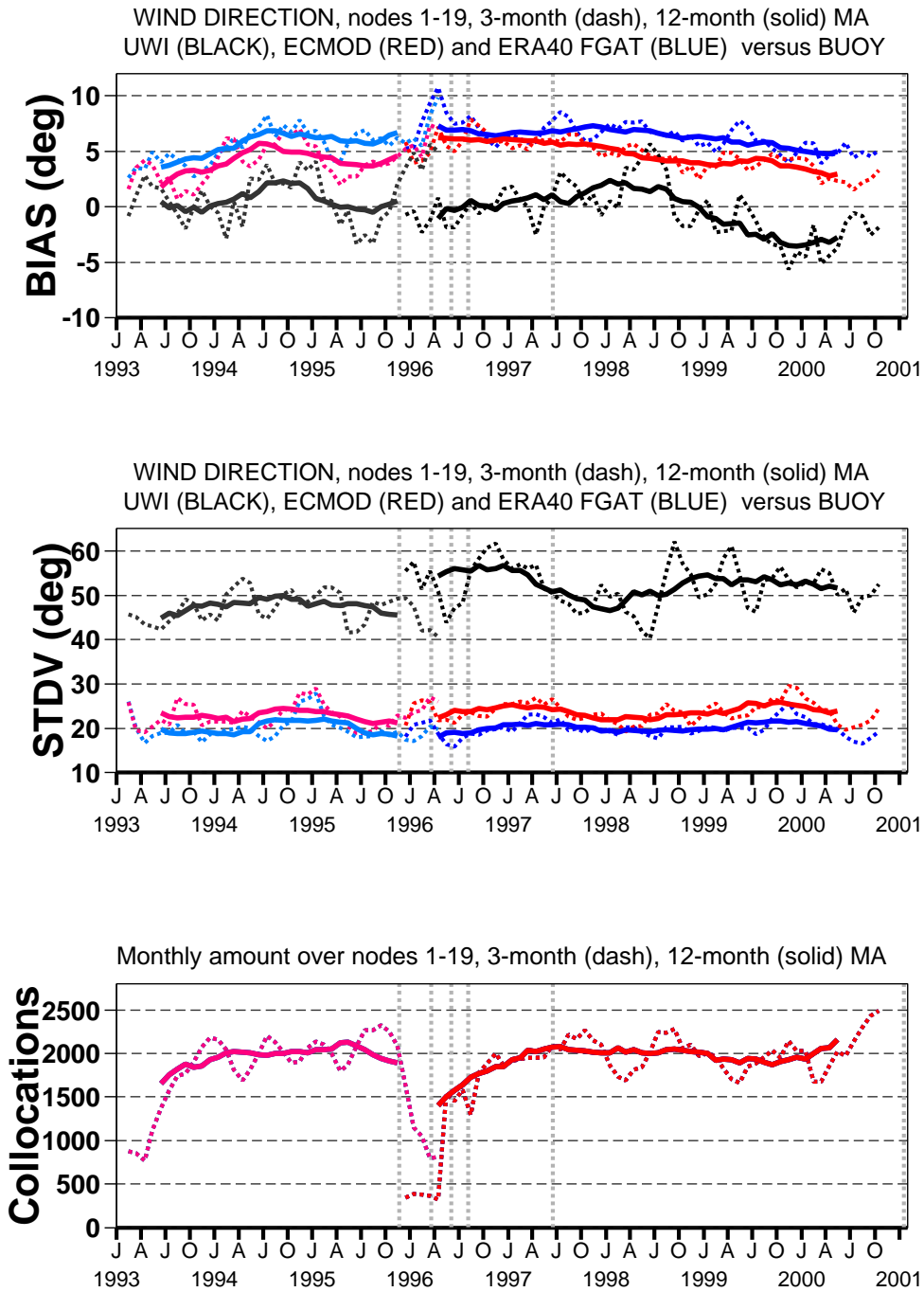


Figure 38: Top and middle panel as for Figure 37, but now for wind direction, and number of triple collocations per month in lower panel.

It is common practise to assume that the buoy observations are unbiased. In case this assumption is used, it follows UWI winds are, on average, about 0.9 ms^{-1} biased low for ERS-2 and 0.8 ms^{-1} for ERS-1. The strong time-dependency during the pre-calibration period of ERS-2 (22 November 1996 to 19 March 1996) is a reflection of variation in the level 1B calibration, since such variations are hardly present for the corrected ECMOD winds (red). However, significantly different bias levels are found for those winds between ERS-1 and ERS-2. It indicates a non-optimal tuning of the applied bias corrections. During the period in which the redundant calibration sub-system had been used (6 August 1996 to 18 June 1997), a trend is observed in bias levels for both the UWI and ECMOD product (also indicating a non-optimal correction for ECMOD). During the nominal period (18 June 1997 to 17 January 2001) bias levels are stable. For the ERA-40 FGAT winds the long-term bias is flat, however, being more negative ($\sim 0.4 \text{ ms}^{-1}$) during the ERS-1 period than during the ERS-2 period ($\sim -0.2 \text{ ms}^{-1}$). Although this might be a reflection of the changing observation system (e.g., the switch of assimilating from ERS-1 to ERS-2 itself), changing properties in the buoy observational network cannot be ruled out either.

Note that the seasonal fluctuations in bias, as discussed in Section 5.4, are clearly visible within the entire ERS-1 and ERS-2 record. The fluctuations in the relative bias for the UWI and ECMOD winds are, at least partly, due to the difference between the (neutral) scatterometer winds and non-neutral buoy winds. Yearly variations in the (also non-neutral) ERA-40 FGAT winds, however, are realistic, and show that during (Northern-Hemispheric) Summer, ECMWF model winds are biased low the most. Since these concern on average stable conditions (versus unstable conditions during winter), this seems to confirm a dependency of the ECMWF surface wind bias on atmospheric stability, as was, e.g. conjectured in Figure 35.

As emerges from the top panel of Figure 37, seasonal fluctuations in bias are averaged out effectively by yearly averaging. Therefore, buoy collocation studies should preferably embrace an integer number of years.

Time-series for standard deviation in wind speed relative to buoy are displayed in the middle panel of Figure 37. It shows that the large values for UWI during the ERS-2 pre-calibration phase are not present for the properly corrected ECMOD winds. In general, the standard deviation of the ECMOD winds are somewhat lower than for UWI, and, therefore, indicate the potential quality of the AMI instrument. Largest deviation from the buoys is found for the ERA-40 FGAT winds. Part of this error, however, probably arises from the large difference in the temporal and spatial scales represented by the two wind sources. Random relative errors are smaller during the ERS-1 period than during the ERS-2 period for UWI, ECMOD, and ERA-40 FGAT. This would suggest that the AMI on-board ERS-1 was the more accurate one. However, the error in the ERA-40 FGAT wind should not be higher (by 0.2 ms^{-1}) for the ERS-2 period.

A way to disentangle this issue is to estimate the error of each system separately. In case three sets of observations, say X , Y and Z , are available, and if these sets are mutually independent, then this, indeed, appears possible. The random error of each subset σ_X , σ_Y and σ_Z , can then be estimated from the (observed) relative error σ_{X-Y} between set X and Y , and other combinations, by:

$$\left. \begin{aligned} \sigma_{X-Y}^2 &= \sigma_X^2 + \sigma_Y^2 \\ \sigma_{Y-Z}^2 &= \sigma_Y^2 + \sigma_Z^2 \\ \sigma_{Z-X}^2 &= \sigma_Z^2 + \sigma_X^2 \end{aligned} \right\} \implies \sigma_X^2 = \frac{1}{2} (\sigma_{X-Y}^2 + \sigma_{Z-X}^2 - \sigma_{Y-Z}^2) \quad (1)$$

For the present collocation set, such triples are available, e.g., ECMOD, ERA-40 FGAT and buoy. The difference in represented scales between the three sets will introduce correlations, though. Since largest mismatch in scale occurs for the ERA-40 FGAT winds, the three sets can still be regarded as independent, however, with the price that most representativeness errors will be absorbed by the model winds. The results are displayed in the lower panel of Figure 37. From this it appears that, for at least the first three years of the ERS-2 period, the

buoy network is of lower quality than it is during the ERS-1 period. This explains the apparent lower relative errors in the middle panel of Figure 37 during the ERS-1 period. In fact, it now emerges that the error of the ERA-40 FGAT winds is comparable across both periods. In particular, the error of the ECMOD wind now appears very stable, and on the same low level of $\sim 0.6 \text{ m s}^{-1}$ for both ERS-1 and ERS-2 periods. An analysis with replacement of the ECMOD winds by UWI winds gives very similar results for the ECMWF FGAT and buoy error, though with a slightly increased UWI error ($\sim 0.7 \text{ m s}^{-1}$, not shown).

To summarize, the triple-collocation analysis indicates that the quality in wind speed from both ERS-1 and ERS-2 AMI instruments is similar, stable, and high.

Statistics for wind direction are presented in Figure 38. For relative bias (top panel) it is found that ERA-40 FGAT winds are about two degrees biased clock-wise compared to ECMOD winds. It represents the lack of the previously described cross-isobar flow (Hollingsworth 1994, Brown *et al.* 2005), as e.g., visible for typhoon Saola in the left panel of Figure 32. However, it appears that the biases compared to the buoy wind direction are in the order of 5 degrees. It slowly involves in time, and is largest for the first few years of the ERS-2 period. Although the reason for this bias is not known, a similar relative bias for NSCAT versus NDBC buoys was observed by Freilich and Dunbar (1999). For TAO buoys, a firmware bias of 6.8 degrees is known to exist (TAO, 2005), however, the present study nor the study by Freilich and Dunbar (1999) involved such tropical buoys.

Wind direction for the UWI product is more unbiased, however, due to the large fraction of incorrect de-aliasing, this quantity is somewhat meaningless. This is seen from the middle panel of Figure 38, where the relative STDV of the UWI wind is much higher than that for properly de-aliased ECMOD winds. The difference in level, indicates that the de-aliasing of the UWI product had a higher success rate for ERS-1 than for ERS-2. The quality of the de-aliased ECMOD wind direction is very stable over the entire ERS era, and scatter is somewhat higher than for ERA-40 FGAT wind.

5.6 Post-calibration of Geophysical model function CMOD5

A comparison between routine monitoring of CMOD5 versus FGAT and QuikSCAT versus FGAT winds (see e.g., Figure 33) shows that CMOD5 winds are about 0.5 m s^{-1} slower than QuikSCAT winds. A one-year (1 August 1998 to 31 July 1999) triple collocation study with NDBC buoy data was performed in similar manner as described in the previous Section. From this a negative bias of 0.45 m s^{-1} did indeed emerge. In addition the bias appears to be quite constant over the wind speed range. A refit of the 28 coefficients of CMOD5 was performed to correct for this bias. At the time of this writing, however, results are still preliminary, and details will be recorded at a later stage.

5.7 Validation of reprocessed UWI data

Currently, reprocessing activities for ERS-1 and ERS-2 scatterometer data are taking place at ESRIN (Crapolicchio *et al.*, 2004). Reprocessing is done from level 0, using a specially designed data (re)processor (called ASP20). In addition to a (nominal NRES) 25 km product, a 12.5 km product (HRES) is to be created. Objectives are

- to obtain a well-calibrated, homogeneous level 1B (backscatter triplets) product, throughout the entire ERS-1 and ERS-2 archive.
- to include data that had not met the operational dissemination cut-off slot.

- to include, and correct, the data-void period from January 2001 to August 2003
- to provide a level 2 wind product based on CMOD5, containing up to four wind solutions, in contrast to the single solution in the operational UWI product.
- to add information on sea-ice, and provide enhanced information on quality control in general.

During the 27th ASCAT SAG meeting (6-7 April 2005) two DVD-ROM's were distributed containing test data for Cycle 43 (25 May - 28 June 1999) produced by ASP515; the at that time latest version of the reprocessor. Among other differences, winds had been inverted on the basis of CMOD4, rather than CMOD5. SAG members were invited to test its contents. At ECMWF, data for 15 June 1999 was collocated with archived UWI data as it had been assimilated at ECMWF. In this way, differences between the reprocessed and the operational UWI product could be studied efficiently. Also, such archived FEEDBACK files contain well-collocated ECMWF FGAT winds, which enables assessment of data quality as well. The reprocessed data is presented in unformatted IDL output. Since it appeared difficult to read this data into Fortran, a small IDL routine was used to dump data to ASCII. These files were then collocated with UWI BUFR files, using the ECMWF collocation package. Collocation limits between the two data sets were set to 5 minutes and 15 km. Both HRES and NRES data were regarded.

5.7.1 Comparison with operational UWI winds

For the NRES product, one wind solution was usually found to be very similar to the wind recorded in the UWI product. Relative bias in wind speed was small (NRES winds are 0.03 ms^{-1} weaker than UWI) and the scatter was low ($\sim 0.3 \text{ ms}^{-1}$). Largest deviations were found for winds between 5 and 10 ms^{-1} . For wind direction, some noticeable deviations were found, with a relative standard deviation of 10 degrees (i.e., about half of the standard deviation between UWI and FGAT winds). For HRES data differences were larger. The reason for this, obviously, is the difference in resolution. Scatter diagrams between UWI winds and the closest HRES solution are presented in the top panels of Figure 39. Differences in wind speed are in general small (STDV= 0.49 ms^{-1} , and with HRES 0.06 ms^{-1} weaker). For wind direction, differences are larger (STDV= 12.7 degrees), and are concentrated around angles of 45, 135, 225 and 315 degrees (see top right panel of Figure 39).

5.7.2 Comparison with ECMWF FGAT winds

The question arises whether the reprocessed data are of higher quality. An indication can be obtained by comparing both the reprocessed and operational UWI product with ECMWF FGAT winds. It appears (not shown) that for NRES winds, there is slightly more scatter in wind speed (1.50 ms^{-1} versus 1.48 ms^{-1}), but the quality of the de-aliased wind direction (for the operational UWI winds the second wind solutions is determined at ECMWF, using CMOD4) seems higher (17.0 versus 18.3 degrees). Success rate for the selected wind solution (i.e., for operational UWI the only reported one) is very similar (59% versus 58%).

Again, for HRES data, larger scatter is obtained (see middle and lower panels of Figure 39). Scatter compared to FGAT winds is 1.56 ms^{-1} (versus 1.50 ms^{-1} for operational UWI) in wind speed and 18.8 degrees (versus 18.2 degrees for operational UWI) in wind direction. This result was to be expected for two reasons. First of all, the HRES are defined on a finer grid, which induces (small) collocation errors compared to the FGAT-UWI pairs that are perfectly collocated by definition. Secondly, level 1B HRES data is determined from smaller areas, which induces more noise, and, therefore, more scatter.

To conclude, differences between the operational UWI data and reprocessed data are found to be small. The quality of both sets is comparable. A more in-depth analysis with preferably data from ASP20 is to be

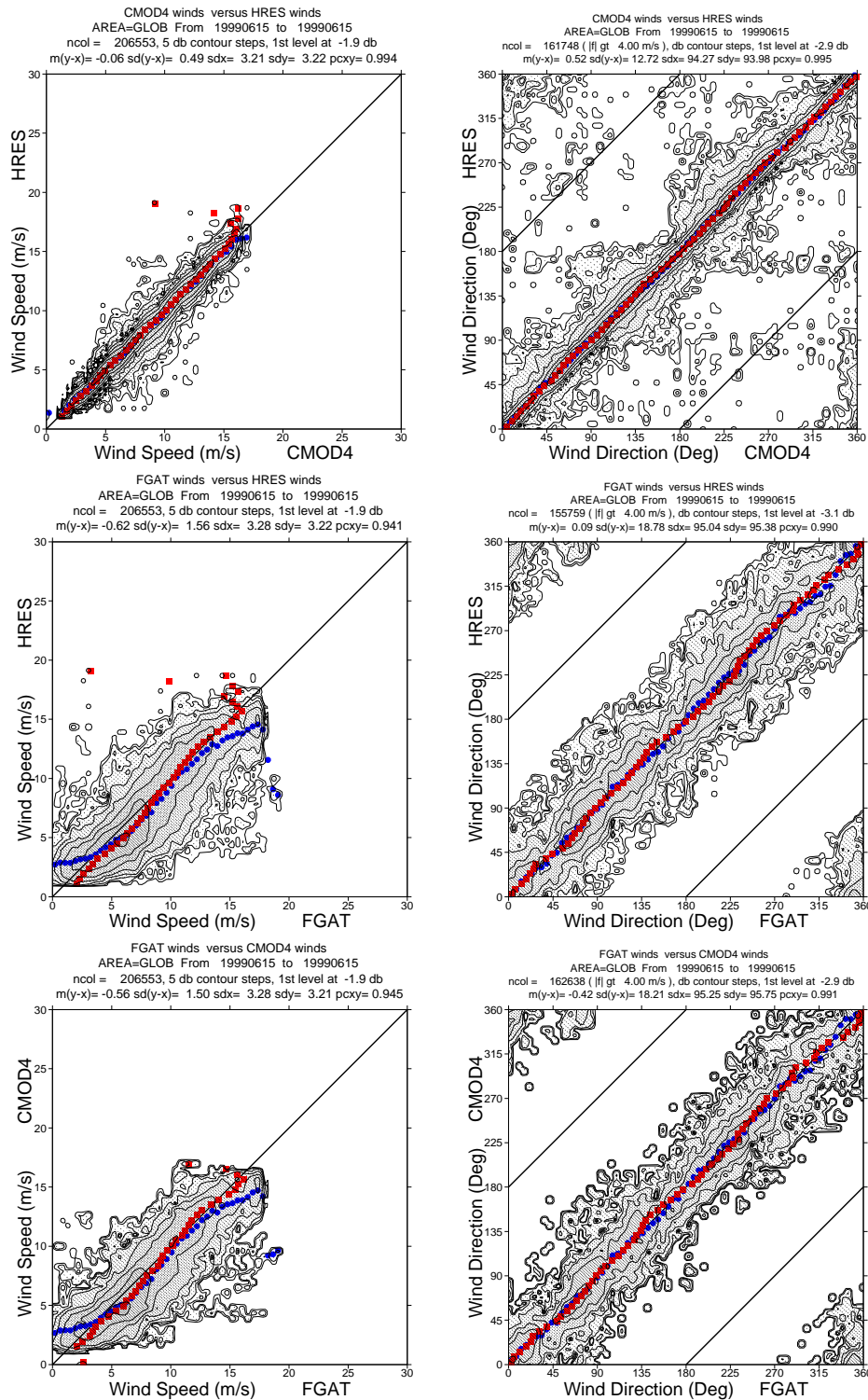


Figure 39: Collocation of HRES reprocessed scatterometer data with the NRT UWI product. Blue circles denote averages for bins in the x-direction, and red squares averages for bins in the y-direction.

performed in the coming year, where besides overall comparison, it is to be investigated whether reprocessed data outperforms operational UWI data for periods of known anomalous behaviour.

6 Concluding remarks

Continuous monitoring and verification of the ERS-2 fast delivery wind and wave products from RA (URA), SAR (UWA) and scatterometer (UWI) are carried out routinely at ECMWF. Data from ECMWF atmospheric (IFS) and wave (ECWAM) models and from in-situ buoy observations are used for this purpose. As a result of the loss of gyros in early 2001, several products were degraded. The main victim was the UWI product, which became of poor quality forcing ESA to halt its dissemination. ESA managed to improve the quality of the UWI product which culminated in the public re-dissemination on 21 August 2003. The quality of the UWI product has been closely monitored at ECMWF since 12 December 2001. On 8 March 2004 ERS-2 scatterometer data was reintroduced at the ECMWF assimilation system. The degradation impact of zero-gyro mode was less pronounced on the URA and UWA products. Since the failure of the ERS-2 low bit rate tape recorders on 22 June 2003, data coverage has been restricted to the North Atlantic and western coasts of North America. More ground stations were later utilized to extend the coverage to the Southern Ocean and the eastern coasts of China. Despite the lack of the global coverage of LBR ERS-2 data, the remaining coverage represents an important area for many applications. Even positive impact on global forecast skill was found in several assimilation experiments (Hersbach 2004a), which led to the re-introduction of the usage of ERS scatterometer data at ECMWF on 8 March 2004. Among others, for these reasons maximum possible continuation of the ERS-2 mission is important.

Long-term evaluation of ERS wind and wave products was carried out for the whole lifetimes of both ERS-1 and ERS-2 missions. Offline altimeter ocean product (OPR) and fast delivery products from SAR (UWA) and scatterometer (UWI) were evaluated and the following results were obtained:

- OPR SWH products from both satellites are of good quality. ERS-2 SWH product is about 30 cm higher than ERS-1. It seems, however, that ERS-1 SWH product is slightly better than ERS-2 product.
- The OPR wind speed product had several problems by time. ERS-1 OPR wind product suffered significant abrupt changes in bias at least 3 times. On the other hand, ERS-2 OPR wind speed product was rather stable for the first 4.5 years before it started to degrade (especially in the Southern Hemisphere) after the gyro problems started in early 2000. Therefore, one should handle the altimeter wind speed product with care especially for climate studies.
- SWH from ERS-1 UWA product is too high with respect to the wave model with at least two significant jumps in bias. The product seems to be degraded during Phase G (after March 1995). On the other hand, ERS-2 UWA product seems to be much better with lower bias and standard difference with respect to the wave model. However, a calibration bug (July 1998-November 2000), the loss of the gyros (January-June 2001) and the loss of the global coverage (starting from June 2003 onwards) are all degraded the product (or its inversion) during most of ERS-2 lifetime.
- The quality of the operationally disseminated UWI wind product is in principle high, stable and comparable for ERS-1 and ERS-2. A triple collocation study with ECMWF reanalysis and buoy winds indicates an intrinsic random error of $\sim 0.6 \text{ m s}^{-1}$. On average, the UWI wind speed is about 0.9 m s^{-1} biased low compared to the buoy observations. The potential quality (i.e., after proper de-aliasing) in wind direction is similar between both platforms as well, though for ERS-2 more often the incorrect wind solution is reported.

Basic analysis on test data from the reprocessing activities at ESRIN for UWI data gave satisfactory results. The following recommendation can be formulated:

- The current data format (unformatted output from IDL scripts) appears not very portable. Another, more standardized and portable format, such as BUFR, would be preferable.
- The data-void period (January 2001 - August 2003) should be reprocessed first. Not only will this fill the gap in the UWI history, it will also provide an excellent quality test for reprocessed data during this anomalous period.

Monthly or cyclic monitoring reports can be found at:

URA (monthly): <http://earth.esa.int/pcs/ers/ra/reports/ecmwf>

UWA (monthly): <http://earth.esa.int/pcs/ers/sar/reports/ecmwf> (password protected)

UWI (5-weekly): <http://earth.esa.int/pcs/ers/scatt/reports/ecmwf>

Acknowledgements

The work presented in this paper was funded by ESRIN (Project Ref. 18212/04/I-OL). We would like to thank Peter Janssen, Jean-Raymond Bidlot, Lars Isaksen and Raffaele Crapolicchio, for support and valuable discussions. Conversion of OPR products into BUFR and the wave model hindcast using ERA-40 wind fields which was used for OPR wave product verification were carried out by Jean-Raymond Bidlot.

A Appendix: Related Model Changes

Note: All changes were introduced for the 6-hour time-window centred at 18:00 UTC.

21 Jun. 1992 Operational implementation of the global model on a 3 degree latitude-longitude grid (63°S to 72°N). The wave spectrum is discretized using 12 directions and 25 frequencies (from 0.041772Hz).

15 Aug. 1993 Assimilation of ERS-1 RA wave heights in global model.

3 Jul. 1994 The global model horizontal resolution was increased to 1.5 degree (from 81°N to 81°S).

19 Sep. 1995 New windsea/swell separation scheme.

30 Jan. 1996 Changes to IFS (e.g. 3DVAR operational).

1 May 1996 Assimilation switch from ERS-1 to ERS-2 RA wave heights.

1 Jun. 1996 Changes to IFS to switch the assimilation of scatterometer winds from ERS-1 to ERS-2.

4 Dec. 1996 The global model horizontal resolution was changed to a 0.5 irregular latitude-longitude grid, with an effective resolution of about 55 km (from 81°N to 81°S). Change the wave-model integration scheme to accommodate Hersbach and Janssen new limiter.

13 May 1997 Modification of the advection scheme by defining the first direction as half the directional bin.

27 Aug. 1997 Changes to IFS (e.g. scatterometer winds are no longer blacklisted for speeds above 20 m/s and modification to the scatterometer bias).

- 11 Nov. 1997** Changes to IFS (e.g. modification of the scatterometer QC).
- 25 Nov. 1997** Changes to IFS to implement the 4D-Var assimilation scheme.
- 1 Apr. 1998** Changes to IFS model (e.g. change horizontal resolution to T319).
- 28 Jun. 1998** Operational implementation of the coupling between WAM and IFS.
- 9 Mar. 1999** 10 m winds are used in coupled model. IFS changes (e.g. change vertical resolution to 50 levels, and modification of the scatterometer QC).
- 13 Jul. 1999** RA wave height correction based on non-gaussianity of the sea surface elevation. Change to the frequency cut-off in the integration scheme. IFS changes (new physics/dynamics coupling).
- 12 Oct. 1999** Changes to IFS model (e.g. change vertical resolution to 60 levels, and new orography)
- 11 Apr. 2000** RA data quality control based on peakiness factor. Penalization of low altimeter wave heights in data assimilation. An extra iterative loop to determine the surface stress.
- 27 Jun. 2000** Sea ice fraction is used for the ice mask. The buoy validation software was upgraded to use the proper anemometer height.
- 11 Sep. 2000** Assimilation scheme in IFS changed to 12 hour 4D-Var.
- 20 Nov. 2000** Increase the horizontal resolution of the atmospheric model to T511 (around 40 km). Increase spectral resolution in the global deterministic WAM model to 24 directions and 30 frequencies. Improved advection scheme on irregular grids. New empirical growth curves in the RA data assimilation. Bug fix of the SAR inversion software to properly use SAR data with the new calibration procedure (the bug was effective since June 1998).
- 11 Jun. 2001** IFS modifications.
- 21 Jan. 2002** Modified scheme for the time integration of the source terms. Assimilation of QuikSCAT data in IFS model.
- 8 Apr. 2002** Inclusion of wind gustiness and air density effect. Removal of spurious values for the Charnock parameter. Blacklisting procedure for wave data.
- 16 Apr. 2002** Extra quality control for QuikSCAT.
- 13 Jan. 2003** Assimilation of ERS-2 SAR data. Background check for altimeter data during assimilation. Significant changes to IFS model, including a new minimisation scheme and improved background error in the assimilation part.
- 22 Oct. 2003** Assimilation of ENVISAT Radar Altimeter-2 Ku-Band significant wave heights. ERS-2 RA wave height assimilation was discontinued. (This change was introduced at 6-hour time-window centred at 00:00 UTC.)
- 8 Mar. 2004** Use of unresolved bathymetry in wave model. Wave model is now driven by neutral 10-metre wind. Re-introduction of ERS-2 scatterometer data based on CMOD5.
- 28 Jun. 2004** The implementation of the early delivery system.
- 27 Sep. 2004** Proper treatment of the initialisation of wave fields for time windows 06:00 and 18:00 UTC.
- 5 Oct. 2004** Stop erroneously discarding some ENVISAT altimeter data in wave analysis.
- 5 Apr. 2005** Implementation of a revised formulation for ocean wave dissipation due to wave breaking.

1 Feb. 2006 Implementation of the high resolution atmospheric (T799) and wave (0.36°) models. ENVISAT ASAR Level 1b Wave Mode spectra replaced ERS-2 SAR in assimilation. Jason altimeter wave height data are assimilated.

References

Abdalla S. and Hersbach H. (2004). The technical support for global validation of ERS Wind and Wave Products at ECMWF, *Final report for ESA contract 15988/02/I-LG*, ECMWF, Shinfi eld Park, Reading. http://www.ecmwf.int/publications/library/ecpublications/_pdf/esa/ESA_abdalla_hersbach.pdf

Attema, E., P., W. (1986). An experimental campaign for the determination of the radar signature of the ocean at C-band, *Proc. Third International Colloquium on Spectral Signatures of Objects in Remote Sensing*, Les Arcs, France, ESA, SP-247, 791-799, 1986.

Bidlot, J. R., D. J. Holmes, P. A. Wittmann, R. Lalbeharry, H. S. Chen (2002). Intercomparison of the performance of operational ocean wave forecasting systems with buoy data. *Wea. Forecasting*, **17**, 287-310.

Bidlot, J. R., Janssen, P. A. E. M., Abdalla, S. (2006). Impact of the revised formulation for ocean wave dissipation on ECMWF operational wave models. *ECMWF Technical Memorandum (In preparation)*.

Brown, A. R., Beljaars, A. C. M., Hersbach, H., Hollingsworth, A., Miller, M., Vasiljevic, D. (2005). Wind turning across the marine atmospheric boundary layer *Quart. J. Roy. Meteor. Soc.* **607**, 233-1250.

Brown, A. R., Beljaars, A. C. M., Hersbach, H. (2006). Errors in parametrizations of convective boundary layer turbulent moment mixing *Accepted for publication in: Quart. J. Roy. Meteor. Soc.*

Crapolicchio, R., P. Lecomte, X. Neyt (2004). The advanced scatterometer processing system for ERS data: design, products and performance. Proceedings of the ENVISAT and ERS Symposium, Salzburg, Austria, 6-10 September 2004.

ESA (2005). ERS-1 Mission Phases (from 1991 onwards). *An Internet web page* accessible from: <http://earth.esa.int/rootcollection/eo/ERS1.1.7.html>
Last visited: 21 July 2006.

Féménias P., and Martini A. (2000). ERS-2 AOCS mono-gyro attitude software Qualification Period - Radar Altimeter Data Analysis. *ESA-ESRIN Technical Note*, accessible from: <http://earth.esa.int/pcs/ers/ra/events/monogyro/>

Freilich, M. H., and Dunbar R. S. (1999). The accuracy of the NSCAT 1 vector winds: comparisons with National Data Buoy Center buoys, *J. Geophys. Res.*, **104 (C5)**, 11,231-11,246.

Hersbach, H. (2003). CMOD5. An improved geophysical model function. *ECMWF Technical memorandum 395*, ECMWF, Reading, England.

Hersbach H., Janssen P. A. E. M., Isaksen, L. (2004a). Re-introduction of ERS-2 scatterometer data in the operational ECMWF assimilation system. Proceedings of the ENVISAT and ERS Symposium, Salzburg, Austria, 6-10 September 2004.

Hersbach H., Stoffelen A., Haan de S. (2004b). The improved C-band geophysical model function CMOD5. Proceedings of the ENVISAT and ERS Symposium, Salzburg, Austria, 6-10 September 2004.

IFS documentation, (2004). edited by P. White, <http://www.ecmwf.int/research/ifsdocs/CY28r1/>

Isaksen, L., and Janssen P. A. E. M. (2004). The benefit of ERS Scatterometer Winds in ECMWF's variational assimilation system. *Q. J. R. Meteorol. Soc.* **130** 1793-1814,

Janssen, P. A. E. M. (2004). *The interaction of ocean waves and wind.*, Cambridge Univ. Press, 300p.

Janssen, P. A. E. M., B. Hansen, Bidlot J. R. (1997). Verification of the ECMWF wave forecasting system against buoy and altimeter data, *Wea. Forecasting*, **12**, 763-784.

Janssen, P., Bidlot, J. R., Abdalla, S., Hersbach H. (2005). Progress in Ocean Wave Forecasting at ECMWF. *ECMWF Technical Memorandum 478*, ECMWF, Reading, UK. Available online from: http://www.ecmwf.int/publications/library/ecpublications/_pdf/tm/401-500/tm478.pdf

Stoffelen, A. C. M., and Anderson D. L. T. (1997). Scatterometer Data Interpretation: Derivation of the Transfer Function CMOD4, *J. Geophys. Res.*, **102** (C3) 5,767-5,780.

TAO (2005) Tropical Atmosphere Ocean project, Sensor specifications. Web page

http://www.pmel.noaa.gov/tao/proj_over/sensors.shtml

Last visited 1 August 2006.

Uppala, S. M., Kållberg, P. W., Simmons, A. J., Andrae, U., Da Costa Bechtold, V., Fiorino, M., Gibson, J. K., Haseler, J., Hernandez, A., Kelly, G. A., Li, X., Onogi, K., Saarinen, S., Sokka, N., Allan, R. P., Andersson, E., Arpe, K., Balmaseda, M. A., Beljaars, A. C. M., Van De Berg, L., Bidlot, J., Bormann, N., Caires, S., Chevallier, F., Dethof, A., Dragosavac, M., Fisher, M., Fuentes, M., Hagemann, S.; Hólm, E., Hoskins, B. J., Isaksen, L., Janssen, P. A. E. M., Jenne, R., McNally, A. P., Mahfouf, J. F., Morcrette, J. J., Rayner, N. A., Saunders, R. W., Simon, P., Sterl, A., Trenberth, K. E., Untch, A., Vasiljevic, D., Viterbo, P., Woollen, J. (2005). The ERA-40 re-analysis *Quart. J. Roy. Meteor. Soc.* **131**, 2961-3012.